A SURVEY OF MEASUREMENTS, MODELS, AND EXPLANATIONS OF THE EFFECT OF NANOPARTICLES ON THE SPECIFIC HEAT OF VARIOUS NANOFLUIDS

A Thesis

by

XIAOWAN SHAN

Submitted to the Office of Graduate and Professional Studies of
Texas A&M University
in partial fulfillment of the requirements for the degree of

MASTER OF SCIENCE

Chair of Committee,	Thomas R. Lalk
Committee Members,	Michael Schuller
	Andrew Comech
Head of Department,	Andreas A. Polycarpou

December 2014

Major Subject: Mechanical Engineering

ABSTRACT

A survey was conducted to determine if any unified models and/or explanations exist that adequately predict the change in specific heat of a nanofluid as a function of concentration of nanoparticles.

The papers and previous studies about the specific heat of nanofluids were collected and reviewed. The existing models and experimental data were summarized and compared. Through the investigation, only four different models were discovered, and two types of experimental result of the specific heat of nanofluids were found. Then, the four models were used to predict the change of the specific heat of nanofluids and compare with different selected sets of experimental result. This was intended to determine if the models are suitable for predicting the results of different sets of published results. The published results can be categorized into two types: a decrease in specific heat resulted from the addition of nanoparticles; and an initial increase in specific heat as nanoparticles were added followed by a decrease as the concentration of particles was increased above a particular value. The comparisons showed that there is no unified model that can predict or theory that can explain all the experimental results.

The mechanisms of the enhancement of the specific heat of nanofluids were presented. The results indicated that the enhancement of the specific heat of nanofluids was caused by the high specific surface area of nanoparticles. The specific surface area is a property of a material which is the total surface area of a material per unit of mass. A

higher specific surface area of a material results in an increase of the heat transfer velocity between the material and surroundings.

Further, two novel explanations of the change in the specific heat at a nanoscale level have been proposed. Additionally, suggestions at a nanoscale level for future research of the specific heat of nanofluids have been recommended.

DEDICATION

To my husband

ACKNOWLEDGMENTS

I would like to thank my committee chair, Dr. Thomas Lalk, for his persistent patience and guidance. I also would like to thank my committee members, Dr. Michael Schuller, and Dr. Andrew Comech, for their support and guidance.

I also want to extend my thanks to my friends at Texas A&M University. Their caring and friendships will be one of the most valuable accompanies in my future.

NOMENCLATURE

$C_{p,nf}$	Specific heat of nanofluids
$C_{p,nf}$	Specific heat of nanoparticles
$C_{p,f}$	Specific heat of base fluids
$C_{p,layer}$	Specific heat of nanolayers
$C_{p,m}$	Measured specific heat of nanofluids at a certain particle concentration
$C_{p,c}$	Specific heat of semisolid layers
$\emptyset_{np}$	Volume fraction of nanoparticles
$\emptyset_f$	Volume fraction of a base fluid
ρ_{np}	Density of nanoparticles
ρ_f	Density of base fluids
ρ_c	Density of semisolid layers
W_{nf}, W'_{nf}	Weights of the nanofluid
W_{np}, W'_{np}	Weights of the nanoparticles
W_f, W'_f	Weights of the base fluid
W_{layer}, W'_{layer}	Weights of the nanolayer
α, α'	Mass fractions of the nanoparticles
V_c	Volume fraction of the semisolid layer
V_{np}	Volume fraction of the nanomaterials
V_f	Volume fraction of the base fluid

k, k_f, k_p	Thermal conductivity of nanofluid, base fluid, nanoparticle

TABLE OF CONTENTS

Page

LIST OF FIGURES

Page

LIST OF TABLES

Page

1. INTRODUCTION

In the past few decades, nanofluids have been widely used in many fields such as the electrical, biomedical, and chemical fields. For the U.S industry, nanofluids are used as cooling and heating liquids, which result in conserving 1 trillion Btu of energy [1]. At the Nuclear Science and Engineering Department at MIT, the replacement of cooling water with nanofluids cools down the nuclear power plant significantly faster [1]. Nanofluids can also be used for liquid cooling of computer components in electronic applications. It is predicted that a nanofluid oscillating heat pipe cooling system will be able to remove heat fluxs over $10MW/m^2$. In biomedical applications, an electronically activated drug delivery microchip is delivered by nanodrugs delivery systems.

The various applications of nanofluids, such as those describe above, have been developed due to the advantages they possess. Compared to conventional materials, nanofluids possess many advantages: for example, high specific surface area and more heat transfer surface between particles and fluids, the high dispersion stability, and adjustable properties by varying nanoparticle concentrations to suit different applications [2].

Since nanofluids have so many advantages, scientists have taken great effort in researching their various aspects. For example, thermal conductivity of nanofluids has been widely studied. Most people reached to a unanimity that thermal conductivity of nanofluids increase with particles. Thermal conductivity represents the ability of a material to conduct or transmit heat. The enhanced thermal conductivity of nanofluids

provides higher cooling rates of nanofluids, which is why nanofluids have so many applications as coolants. To achieve a higher heat storage capacity, the specific heat is desired to increase as well, thus, it is meaningful to research on the specific heat.

However, the specific heat of nanofluids was not completely researched to the point where an agreement could be reached on the effects of changing nanoparticle concentrations. It is common to know that putting nanoparticles into base fluids results in a change of nanofluids' specific heat, but it is not known how it changes and why. With continued study of specific heat of nanofluids, the effect of the nanoparticles on the specific heat of base fluids became clear.

To investigate the specific heat of nanofluids, scientists have performed experiments testing the change of specific heat when the temperature, the nanoparticle size, or the particle concentration varies. It is necessary to know the effect of adding nanoparticles into the base fluids. Scientists also developed models and explored theories to explain how and why the specific heat of a nanofluid changes. However, there is no adequate study to show a consistent agreement on the effects of particles on specific heat. Since the published experimental result conflict, the scientists reached no agreement on it. It is necessary to conduct more research to ascertain the effects of particles on the specific heat of nanofluids.

Inspired by the findings of the specific heat of nanofluids, the objective of this research is to determine if there exists (a) unified model(s) and/or explanation(s) that adequately predict and explain all the types of the change in specific heat of a nanofluid as a function of concentration of nanoparticles.

To achieve the above objective, papers and previous studies about nanofluids were surveyed. Then, the papers about the specific heat of nanofluids were organized and screened. The existing models and experimental data were summarized and analyzed to determine if there was a unified model suitable for predicting and explaining published results for the specific heat of nanofluids. Furthermore, the interaction between the nanoparticles and the base fluids at a nanoscale level was investigated in previous studies, and two novel explanations of describing the change of specific heat of nanofluids were proposed. Additionally, several suggestions for further nanofluids' specific heat study were proposed.

This thesis contains eight chapters. The introduction chapter establishes the general interest and specific interest of the thesis, and the general approach of the research, and introduces the outline of the thesis. Before introducing the survey of the specific heat of nanofluids, a Background is necessary to help the audience to better understand the previous studies. Thus, in Chapter 2, several important concepts are introduced such as the concepts of a nanofluid and specific heat. Development of nanoparticles, classification of nanofluids, fabricating methods of nanofluids, and methods of measuring the specific heat of nanofluids are also introduced in Chapter 2. After the Background, the research methods are detailed in Chapter 3. Then, the previous studies of specific heat of nanofluids are shown in Chapter 4. In Chapter 5, an overview and the summarization of the previous experimental data and models of nanofluids' specific heat are presented. The models are compared to different sets of experimental data to verify if they are able to predict all of them. In Chapter 6, the overview of the

explanations of the change of nanofluids' specific heat from the previous studies is presented, and two new explanations describing the change of specific heat of nanofluids from my own perspective are proposed. Chapter 7 contains the findings and the conclusions of the research. Recommendations for future research are given in Chapter 8. All the cited references are listed in the Reference convenience.

2. BACKGROUND

It is necessary to understand some basic knowledge of nanofluids before introducing the research methods and the literature review. Thus, in this chapter the background and concepts of nanofluids and specific heat are introduced. The factors of nanoparticle size, nanoparticle and base fluid materials, and specific heat measurement methods all influence the specific heat of nanofluids. These multiple variables are listed in the surveyed tables, which are used to compare the nanofluids' specific heat under different circumstances. Thus, it is necessary to introduce these in Background.

2.1 Development of nanofluids

A nanofluid is formed by dispersing a certain amount of nano-sized particles, with average sizes below 100nm, into a base fluid. Prior to using nanometer-sized particles, the previous investigations were dispersing millimeter- or micro-sized solids, which is called slurry. In 1961, a Scottish mathematical physicist named James Clerk Maxwell proposed an innovative concept of using nanometer-sized particles due to their high suspension stabilities. The major problem resulting from the use of millimeter- or micro-sized particles was the rapid settling of these particles in fluids. Since Maxwell, scientists have taken great efforts on breaking the limit caused by dispersing millimeter- or micrometer-sized particles in liquids. Thus, in the last 100 years, scientists have made efforts to investigate more effects of adding nanoparticles into various base fluids.

Table 1 shows the comparison between the suspensions and the characteristics of

microparticles and nanoparticles. It is clear to see that the nanometer-sized particles have higher suspension stability than the micro-sized particles. Figure 1 gives a comparison of different sized particles.

Table 1. Comparison of the suspensions of microparticles and nanoparticles [3]

	Microparticles	Nanoparticles
Stability	Settle	Stable(remain in suspension almost indefinitely)
Surface/Volume ratio	1	1,000 times larger than that of microparticles
Conductivity	Low	High
Clog in microchannel	Yes	No
Erosion	Yes	No
Pumping power	Large	Small
Nanoscale phenomena	No	Yes
Size	0.1-10 micrometer	<0.1 micrometer (100 nanometer)

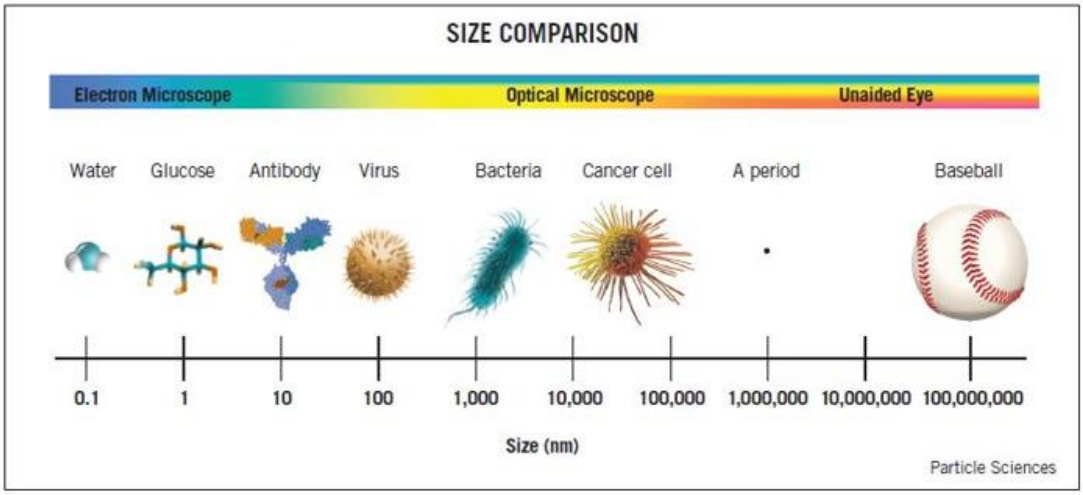

Figure 1. Size comparison [4]

According to several investigation of experimental results, it is clearly pointed

out that the thermal conductivity of nanofluids is enhanced by adding nanoparticles. James Clerk Maxwell also proposed a model that gives a ratio expression of the thermal conductivity of nanofluids to the thermal conductivity of the base fluid for spherical and well dispersed particles. The model is expressed as:

$$\frac{k}{k_f} = \frac{k_p+2k_f+2\emptyset(k_p-k_f)}{k_p+2k_f-\emptyset(k_p-k_f)} \quad (1)$$

However, the research on several other important factors, such as specific heat of nanofluids, particle size and shapes, clustering of particles, and temperature of the base fluids have not been studied as thermal conductivity. Especially for the specific heat, no consensus has been reached in experiments.

2.2 Classification of nanofluids

The types of the nanoparticles and the base fluids are diverse. The nanoparticles are usually made of silica oxide, alumina oxide or zinc oxide, which are produced by chemical or physical synthesis methods such as milling, grinding, and vapor phase methods. Common base fluids include water, ethylene glycol and engine oil. Different combinations of nanoparticles and base fluids lead to different formulations of nanofluids, which results in different characteristics. Table 2 shows different types of nanoparticles and base fluids and their examples.

Table 2. Types and examples of nanoparticles and base fluids

Nanoparticles		Base Fluids	
Types	Examples	Types	Examples
Oxide ceramics	Al_2O_3, CuO	Water	--
Nitride ceramics	AlN, SiN	Oil	--
Carbide ceramics	SiC, TiC	Ethylene glycol	Li_2CO_3:K_2CO_3 (62:38), $NaNO_3$:KNO_3 (60:40), $LiNO_3$:KNO_3 (62:38), K_2CO_3:$CaCO_3$(68:32)
Metals	Cu, Al, Si		
Semiconductors	TiO_2, SiC		
Carbon nanotubes	None reviewed		
Composite materials	$Al_{70}Cu_{30}$	Salt mixture	Chloride salts

2.3 Methods of fabricating nanoparticles and preparing nanofluids

Generally, there are two categories to fabricate nanoparticles: physical processes and chemical processes. Typical physical methods are inert-gas condensation and mechanical grinding. Typical chemical methods include chemical vapor deposition, chemical precipitation, microemulsions, thermal spray, and spray pyrolysis.

There are a number of methods to prepare nanofluids. Most of the nanofluids are made using a two-step process. The first step is preparing the nanoparticles as dry nano-powders and dispersing the nanopowders into a base fluid directly. The second step is adding dispersant addition or ultra-sonication into the mixing liquid to get a nanofluid. An advantage of the two- step process is introducing inert-gas condensation to commercial nanopowder production. The disadvantage is the tendency of nanopowders to agglomerate during dispersion in the base fluids.

By contrast, a one-step method produces better qualified nanofluids than the two-

step method. The one-step method combines the nanoparticle evaporation, condensation and dispersion into one step. Thus, the one-step method saves time, and is able to avoid the cluster of nanoparticles. However, the one-step method is more expensive, and its machine is harder to manufacture. It is also hard for the one-step method to measure and characterize the nanoparticles during the process.

An improvement has been made in the one-step method with better positioning and variable-adjustable distance, which is shown in Figure 2.

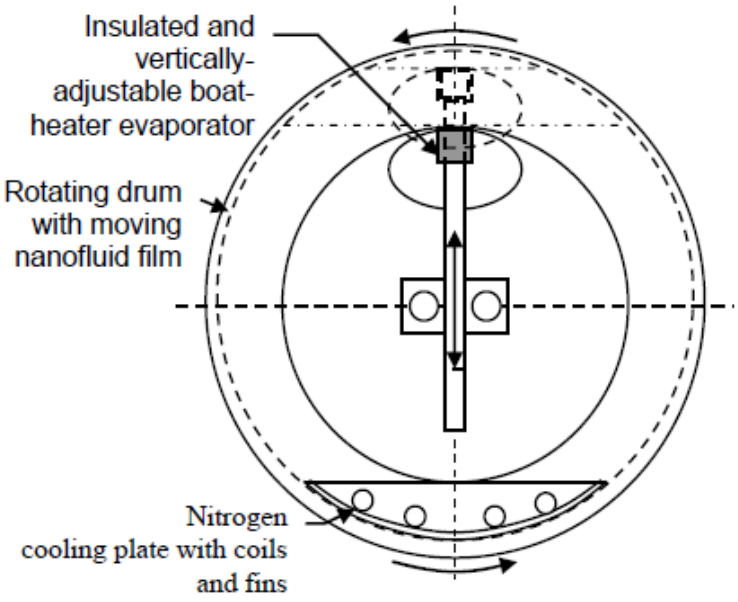

Figure 2. Improved design for the one-step method [5]

2.4 Importance of the specific heat

Specific heat is an important property, and it represents the ability of a material to store energy. Specific heat capacity, also known as “specific heat”, characterizes the energy storage capacity per unit mass of a material, and is a measurable physical

quantity. Specific heat is a property of a particular material. For example, the temperature of the sea is lower than that of the inner land in hot weather, and is higher in cold weather, since water has a higher specific heat than air. The energy of a system is defined by the temperature change, the specific heat and the mass. The expression is shown as equation (2):

$$\Delta E = Cm\Delta T \tag{2}$$

where ΔE is the supplied energy (J), C is the specific heat ($J/kg \cdot K$), m is the mass (kg) and ΔT is the temperature change (K).

Converting equation (2), the specific heat is expressed as:

$$C = \Delta E/m\Delta T \tag{3}$$

Equation (3) indicates that with the same change in the amount of mass and temperature, higher specific heat leads to more stored energy.

2.5 Methods of measuring specific heat of nanofluids

The most commonly used methods to measure the specific heat of nanofluids are differential scanning calorimetry (DSC) and direct-synthesis methods. A sample scanning method using a scanning electron microscope (SEM) is used to track the physical structure of the nanoparticles of a nanofluid.

Differential scanning calorimetry (DSC) is an instrument which uses a thermo-analytical technique to measure the amount of energy required to increase the

temperature of a certain amount of a material to obtain the specific heat value. The DSC was proposed by E. S. Watson and M. J. O'Neil [6]. Figure 3 depicts a schematic of a DSC instrument and Figure 4 is a photograph of a DSC instrument.

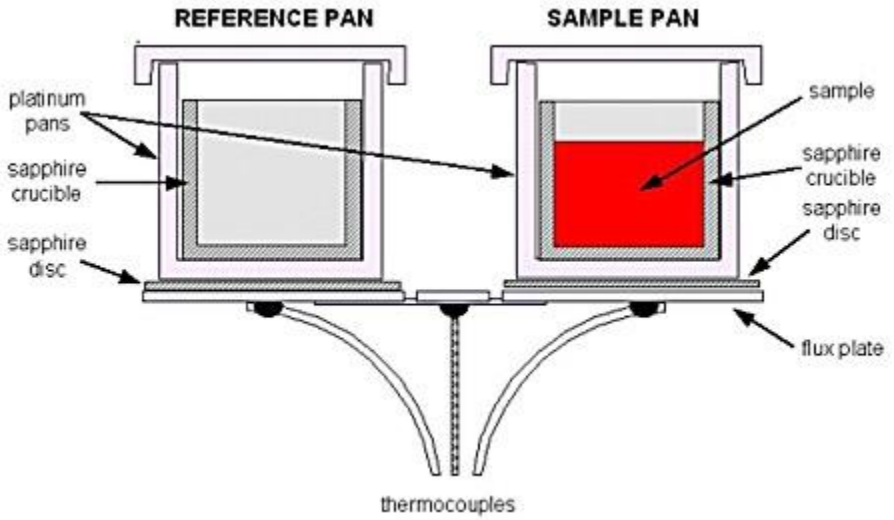

Figure 3. Schematic of a DSC instrument [7]

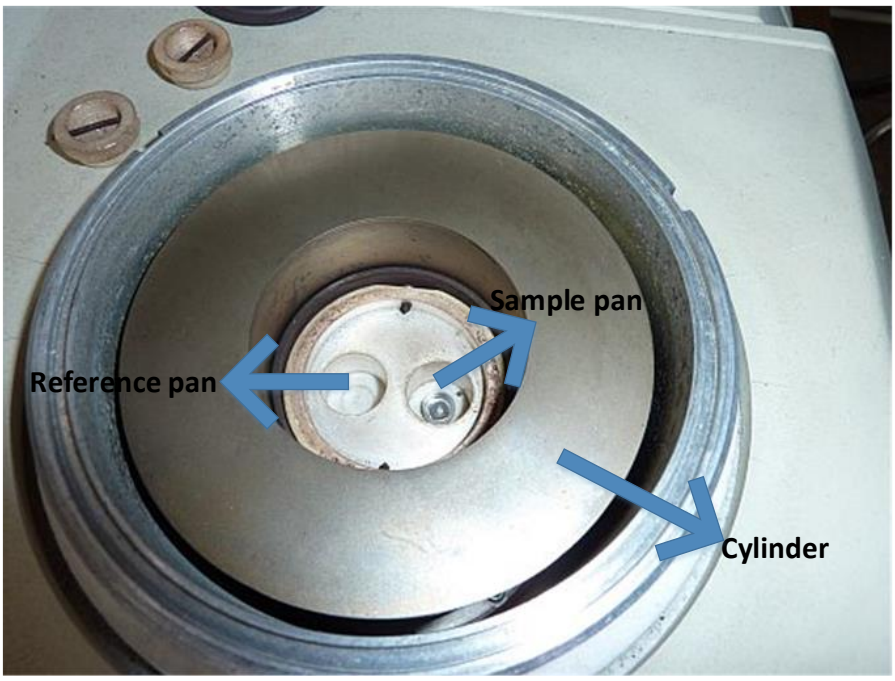

Figure 4. Differential scanning calorimetry instrument [6]

The DSC technique accomplishes measuring the specific heat of nanofluids by comparing the heat flux in two pans with the sample and a reference maintained nearly at the same temperature throughout the experiment. As shown in Figure 3 and 4, a DSC instrument has two pans that are designed to compare the sample and a reference. The temperature for DSC analysis is linear and designed as a function of time.

The classical DSC contains three steps to achieve the goal of specific heat values' measurements. First, two empty sample pans are loaded into a DSC to measure the bias of the DSC instrument. The bias is used to estimate the errors of this instrument and to adjust further measurements. Second, the two empty pans are taken out and two new pans are loaded into the DSC. One of the two new pans contains a reference sample with a known specific heat value; and the other one is empty. Specific heat values of the reference sample are recorded through the defined temperature. Third, a measurement is taken from the actual sample. All three measurements are taken at the same temperature. The heat flux curves of these three measurements are used to comparatively determine the specific heat value of the sample.

Scanning electron microscope (SEM) is a type of electron microscope that can scan the sample with the beam of electrons. Figure 5 is a copy of the photograph which illustrates the equipment of the scanning electron microscope. Its electron beam can focus on a spot with 0.4nm to 5 nm in diameter and energy ranging from 0.2 KeV to 40 KeV. When the primary electron beam interacts with the sample, the electrons will lose energy, and the size of interaction volume will be changed. Next, the energy exchange between the electron beam and the sample that results in electron scattering leads to the

development of images. A scanning electron microscope can produce good qualified image resolution. Figure 6 shows scanned images of several selected nanoparticles used to fabricate the nanofluids through a scanning electron microscope. The images can be saved to a computer data storage device.

Figure 5. Analog type scanning electron microscope in the Geological Survey of Israel Laboratory [8]

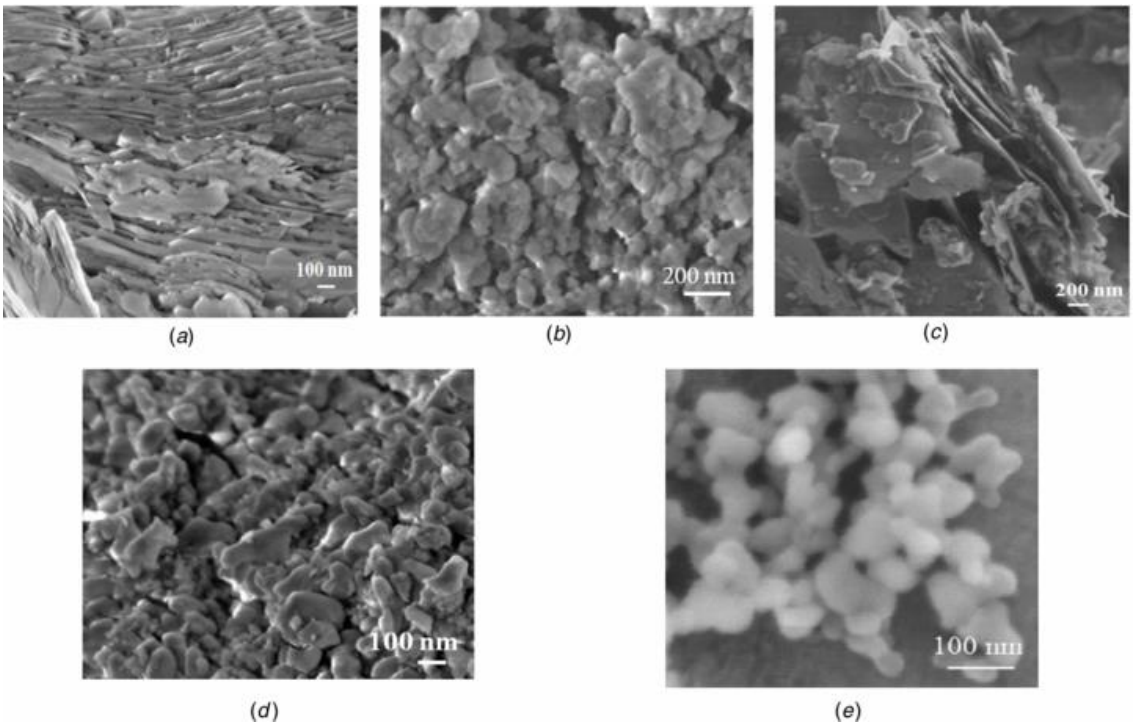

Figure 6. SEM micrographs of (a) clay I, (b) clay II, (c) clay III, (d) Al_2O_3, and (e) CeO_2 nanoparticles used in the fabrication of nanofluids [8]

3. APPROACH

Several methods were used to fulfill the tasks and to accomplish the objective of the project. First, to survey the previous studies about the specific heat of nanofluids, the materials were collected through the website and Evans library. As a result, more than forty papers and three books about nanofluids were downloaded and borrowed. There was another book about the thermal energy transfer at a nanoscale level from Dr. Thomas Lalk. All of these materials were reviewed to choose the ones that provide the models, the explanations, or the experimental data of nanofluids' specific heat.

Second, the selected papers were organized in chronological order to form the literature review, and then it was recognized that there was no agreement on the trends of nanofluid specific heat change. Next, the experimental data of nanofluids' specific heat was categorized into different tables by trends. The trends of the experimental result were easily observed by reading the numbers. In order to illustrate the change of nanofluids' specific heat by adding the nanoparticles, several selected sets of experimental result were evaluated through a simple calculation. Then, the results of the calculation were plotted in figures.

Third, the papers did not provide models were screened out, and those with them were listed in the corresponding tables: each table contains the models that predict the experimental result in one same trend. The tables showed that more than one papers adopted the same models to predict the experimental result. Then, total different models that have been proposed were summarized. Each model was analyzed independently to

determine if any of them was able to adequately predict all the experimental result of the specific heat of nanofluids. To achieve this, for example, the predictions of the models were compared with several different sets of experimental result. Meanwhile, the theoretical explanations from each paper were reviewed and organized to illustrate each trend of the specific heat of nanofluids.

Fourth, references about thermal energy transfer particular at the nanoscale were reviewed to explain the interaction between the nanoparticles and the base fluids at a nanoscale level. It was also effective for proposing novel explanations of the change in specific heat of nanofluids. Based on the findings, several suggestions for future nanofluids' specific heat study were proposed.

4. LITERATURE REVIEW

Since “nanofluid” was first proposed by Choi [9] as a term, its unique characteristics have attracted attention from more and more researchers. The investigation of the specific heat of nanofluids has been carried out through experiments and theories. Models that predict the behaviors of the specific heat of nanofluids have been developed.

The specific heat values of nanofluids are tested by adding different concentrations of nanoparticles in the same base fluid. The models are used to predict the change of the specific heat of nanofluids as a function of the nanoparticle concentrations. In 1998, Pak and Cho [10] dispersed SiO_2 into water and ethylene glycol. The specific heat of the nanofluid is found to be decreased when the nanoparticle concentration increased. Pak and Cho [10] also used a model to precisely predict their experimental result.

In 2007, Namburu et al. [11] found that the specific heat values of SiO_2 nanofluid in ethylene glycol and water decreased as nanoparticles’ volumetric concentration increased. SiO_2 nanoparticles were selected in the experiments due to their economic budget. The experiments showed that with a 10% silicon oxide nanoparticle concentration, the specific heat was about 12% lower than the base fluid.

In 2008, Zhou and Ni [12] investigated a water-based aluminum oxide nanofluid with a differential scanning calorimeter. For example, they discovered that the specific heat of nanofluids decreases gradually as the concentration increases from 0.0% to

21.7%. Zhou and Ni [9] pointed out their experimental result agrees with the prediction from the model.

In 2009, Zhou [13] showed that the 0.1%-0.6% of CuO particles slightly decreased the specific heat values from 2550 to 2450 $kJ/kg \cdot K$. Zhou [13] employed a DSC to measure the specific heat of the nanofluid. The measurements showed that the specific heat values decreased consistently with the increase of nanoparticles. Zhou [10] used a computer model to successfully predict the measurements.

In 2011, Murshed [14] used the transient double hot wire technique to measure several types of nanofluids. The nanofluids were prepared by suspending different volume percentages of TiO_2, Al_2O_3, and Al nanoparticles in ethylene glycol and engine oil. The specific heats of these nanofluids decreased substantially with nanoparticle volume fraction. The prediction from the model showed an agreement with the experimental result. Murshed [14] also demonstrated that the volume fraction, the material and shape of particles, and the type of base fluids influence the specific heat of nanofluids.

In 2011, O'Hanley et al. [15] used a heat-flux-type DSC to measure the specific heat of nanofluids, which decreased with adding nanoparticles. Then they compared their experimental result with Zhou [13]'s model, and found them to agree.

In 2012, Barbés [16] measured the specific heat of nanofluids with a Micro DSC II microcalorimeter. The nanofluid was formed by dispersing Al_2O_3 in water and ethylene glycol. The specific heat of the nanofluid showed a decreasing specific heat of nanofluids as nanoparticles increased. Further, his experimental result was predicted

accurately through the model.

In 2013, Lu and Huang [17] showed that the specific heat of the molten salt-based Al nanofluid decreased as nanoparticles concentration increased. Lu and Huang [17] proposed a new model considering the nanolayer between the nanoparticles and the base fluid. The prediction of the model coincided with their experimental result.

The above-mentioned experimental result show the nanofluid specific heat decreases with the increased nanoparticle concentration. This phenomenon could be explained because the specific heat of nanoparticles lowers that of nanofluids, since the nanoparticles showed smaller specific heat values. However, since 2011, it was found by three different research groups that nanofluid specific heat changes in a different trend along the concentration of nanoparticles.

In 2011, Shin and Banerjee [18] dispersed SiO_2 nanoparticles into pure eutectic of chloride salts to investigate specific heat of the formed nanofluid. The specific heat of the nanofluid was measured at 1% weight concentration of SiO_2 nanofluid, which showed the maximum enhancement of nanofluid around 14.5% in the liquid phase. Shin and Banerjee [18] claimed the traditional models that Zhou and Ni [12], Zhou [13], and O'Hanley et al. [15] used could not explain the anomalous enhancement of the specific heat at such low concentrations of the nanoparticles (0.6% by volume). Shin and Banerjee [18] stated that this anomalous enhancement of the specific heat of the nanofluid demonstrated that alternative transport mechanisms need to be accounted for in the traditional theoretical models. Shin and Banerjee [15] proposed three independent competing inter-molecular interaction mechanisms to explain the unusual enhancement

of the specific heat instead of a theoretical model:

Mechanism I: higher specific surface energy led to enhanced nanoparticle specific heat;

Mechanism II: the interfacial interactions between the nanoparticles and the base fluids led to thermal storage ability of the nanofluid;

Mechanism III: the semi-solid layer between nanoparticles and base fluid had enhanced specific heat.

In 2013, Chieruzzi [19] used four different types of nanoparticles (SiO_2, Al_2O_3, TiO_2 and SiO_2-Al_2O_3) embedded into an identical molten salt base ($NaNO_3$-KNO_3). The nanofluids' specific heat measurements were tested against three nanoparticle concentrations, which were 0.5 wt.%, 1.0 wt.% and 1.5 wt.%. The specific heat values of the four nanofluids all reached the maximum at 1.0 wt.% of nanoparticles. Chieruzzi et al. [19] pointed out that the 1.0 wt.% of SiO_2-Al_2O_3 nanoparticles enhanced the specific heat value by 22.5% in the liquid phase. Chieruzzi et al. [19] did not provide any theoretical model to predict the tested results.

In 2013, Shao [20] reported that the specific heat of the nanofluid showed a parabolic curve within a low concentration of nanoparticles. Shao [20] found out that the addition of Al_2O_3 nanoparticles to nitrate eutectic salts resulted in an increase of the specific heat of the material at first, then a decrease after it reached the maximum value. The maximum specific heat value happened at an optimal concentration of nanoparticles. Shao [20] showed the maximum enhancement of specific heat was 31%, which happened at 0.78 wt.% actual Al_2O_3 mass fraction.

Discussed above are two types of experimental result of specific heat of nanofluids. The first type is that the specific heat of nanofluids decreases when the nanoparticles concentration increases; the second type is that the specific heat of nanofluids reaches its maximum at a low concentration, then decreases consistently. Thus, it is meaningful to determine if there exists a unified model and/or theory to predict and/or explain all the types of experimental result. The analysis of these models is provided below.

5. RESULTS

In this chapter, papers published in recent years about the investigation of specific heat of nanofluids have been reviewed and evaluated. The overviews of all the proposed experimental data and models of the specific heat of nanofluids are presented in tables. The experimental data is listed in Table 3 and Table 4, and the models are listed in Table 5 and Table 6. To analyze the effect of nanoparticles on the base fluids, the percentage changes in the specific heat of various nanofluids as a function of the concentration of nanoparticles are plotted in Figure 7, 8, 9, 10, 11, and 12. This chapter also introduces the comparisons between the predictions of the models and the experimental result.

5.1 Summary of experimental studies on specific heat of nanofluids

By reviewing all the experimental result of specific heat of nanofluilds, two types of experimental result were discovered. The first type is that the specific heat of nanofluids decreases substantially with an increased concentration of nanoparticles; the second type is that the specific heat of nanofluids initially increases, and then decreases as the concentration of nanoparticles increases. Table 3 and Table 4 are created to indicate the two types of experimental data. The first type is contained in Table 3, and the second type is in Table 4.

The concentration of nanoparticles is a key factor in effecting the specific heat of nanofluids. Besides nanoparticle concentration, nanoparticle size, nanoparticle and base

fluid materials, and temperature also influence the specific heat of nanofluids. These multiple variables are listed in Table 3 and Table 4 to compare and evaluate the nanofluids' specific heat under different circumstances. The years of the publications are also listed in Table 3 and Table 4 to track the timeline of the development of nanofluids research.

Some nanofluids are phase change materials. However, in most of these cases, the nanofluids are meant to be used in their liquid phase. The specific heat of nanofluids in the liquid phase is constant, while in the solid phase it increases with temperature. Thus, in Table 3 and Table 4, the specific heat of nanofluids in the liquid phase is recorded.

After the Table 4, the figures that show the ratios of the measured specific heat of nanofluids to the measured specific heat of base fluids are presented in Figure 7-12. This is aimed to clear illustrate the enhancement or decrease caused by nanoparticles of specific heat.

Table 3. Summary of experimental studies on specific heat of nanofluids - I

Author	Year	Base Fluid	Nano-particle	Particle Size (nm)	Nanofluid prepare	*SH Measurements	T (K)	Vol. %	Nanofluid *SH $(kJ/kg \cdot K)$	Uncertainty cited in the publications
Murshed [14]	2011	ethylene glycol	TiO_2	15	---	transient Double Hot-Wire technology	---	0	2.4	±2.1%
								1	2.23	
								2	2.2	
								3	2.15	
								4	2.1	
								5	2.1	
Murshed [14]	2011	deionized water	TiO_2	15	---	transient Double Hot-Wire technology	---	0	4.2	±2.1%
								1	4.0	
								2	3.95	
								3	3.75	
								4	3.65	
								5	3.55	
Murshed [14]	2011	ethylene glycol	TiO_2	10x40	---	transient Double Hot-Wire technology	---	0	2.4	±2.1%
								1	2.21	
								2	2.19	
								3	2.15	
								4	2.1	
								5	2.1	
Murshed [14]	2011	engine oil	Al	80	---	transient Double Hot-Wire technology	---	0	1.9	±2.1%
								1	1.78	
								2	1.76	
								3	1.73	
								4	1.68	
								5	1.63	
Murshed [14]	2011	ethylene glycol	Al	80	---	transient Double Hot-Wire technology	---	0	2.4	±2.1%
								1	2.34	
								2	2.3	
								3	2.28	
								4	2.24	
								5	2.22	

Table 3. continued

Author	Year	Base Fluid	Nano-particle	Particle Size (nm)	Nanofluid prepare	*SH Measurements	T (K)	Vol. %	Nanofluid *SH $(kJ/kg \cdot K)$	Uncertainty cited in the publications
Murshed [14]	2011	ethylene glycol	Al_2O_3	80	---	transient Double Hot-Wire technology	---	0	2.4	$\pm 2.1\%$
								1	2.3	
								2	2.16	
								3	2.09	
								4	2.03	
								5	1.93	
Barbés [15]	2012	water	Al_2O_3	40-50	Two-step method	Micro DSC II microcalorimeter	303.1	1	2.4	not found
								2.5	2.33	
								4	2.25	
								5.8	2.18	
								8.2	2.1	
Barbés [15]	2012	water	Al_2O_3	40-50	Two-step method	Micro DSC II microcalorimeter	330.4	1	2.51	not found
								2.5	2.45	
								4	2.4	
								5.8	2.3	
								8.2	2.2	
Barbés [15]	2012	ethylene glycol	Al_2O_3	40-50	Two-step method	Micro DSC II microcalorimeter	303.1	3.9	3.79	not found
								4.5	2.69	
								5.8	3.59	
								7.5	3.43	
								9.5	3.34	
Barbés [15]	2012	ethylene glycol	Al_2O_3	40-50	Two-step method	Micro DSC II microcalorimeter	330.4	3.9	3.8	not found
								4.5	3.7	
								5.8	3.6	
								7.5	3.45	
								9.5	3.36	

Table 3. continued

Author	Year	Base Fluid	Nano-particle	Particle Size (nm)	Nanofluid prepare	*SH Measurements	T (K)	Vol. %	Nanofluid *SH $(kJ/kg \cdot K)$	Uncertainty cited in the publications
Namburu [11]	2007	ethylene glycol +water	SiO_2	20	---	---	---	0	3.190	not found
								2	3.120	
								4	3.100	
								6	3.040	
								8	2.850	
Zhou et al. [13]	2009	ethylene glycol	CuO	50	---	quasisteady-state method	---	10	2.808	not found
								4	3.100	
								6	3.040	
								8	2.850	
								10	2.808	
								0.6	2450	
Zhou and Ni[12]	2008	water	Al_2O_3	45	---	power compensated DSC	80 ℃	0	4.1707	not found
								2	4.0	
								3.5	3.8	
								7.5	3.5	
								10	3.25	
								12.5	3.125	
								15.8	2.875	
								17.5	2.75	
								21.7	2.37	
Pak and Cho [10]	1998	water	γ-Al_2O_3	13	Two-step method	power compensated DSC	300	1.34	0.675	not found
								2.78	0.745	
								4.33	0.810	
Pak and Cho [10]	1998	water	TiO_2	27	Two-step method	power compensated DSC	300	0.99	0.634	not found
								2.04	0.647	
								3.16	0.662	
								4.35	0.679	

Table 3. continued

Author	Year	Base Fluid	Nano-particle	Particle Size (nm)	Nanofluid prepare	*SH Measurements	T (K)	Vol. %	Nanofluid *SH $(kJ/kg \cdot K)$	Uncertainty cited in the publications
O'Hanley et al. [15]	2011	water	Al	---	---	heat-flux-type DSC	35℃	0.01	3.95	±0.07
								0.015	3.73	
								0.045	3.49	
								0.065	3.4	
O'Hanley et al. [15]	2011	water	Al	---	---	heat-flux-type DSC	45℃	0.01	3.95	±0.07
								0.015	3.73	
								0.045	3.52	
								0.065	3.4	
O'Hanley et al. [15]	2011	water	Al	---	---	heat-flux-type DSC	55℃	0.01	3.95	±0.07
								0.015	3.73	
								0.045	3.55	
								0.065	3.39	
O'Hanley et al. [15]	2011	water	CuO	---	---	heat-flux-type DSC	35℃	0.025	3.64	±0.07
								0.05	3.22	
								0.08	2.76	
								0.13	2.28	
O'Hanley et al. [15]	2011	water	CuO	---	---	heat-flux-type DSC	45℃	0.025	3.61	±0.07
								0.05	3.2	
								0.08	2.7	
								0.13	2.28	
O'Hanley et al. [15]	2011	water	CuO	---	---	heat-flux-type DSC	55℃	0.025	3.61	±0.07
								0.05	3.19	
								0.08	2.62	
								0.13	2.24	
O'Hanley et al. [15]	2011	water	Si	---	---	heat-flux-type DSC	35℃	0.04	3.81	±0.07
								0.085	3.54	
								0.138	3.27	
								0.185	2.95	

Table 3. continued

Author	Year	Base Fluid	Nano-particle	Particle Size (nm)	Nanofluid prepare	*SH Measurements	T (K)	Vol. %	Nanofluid *SH $(kJ/kg \cdot K)$	Uncertainty cited in the publications
O'Hanley et al. [15]	2011	water	Si	---	---	heat-flux-type DSC	45℃	0.04	3.86	±0.07
								0.085	3.56	
								0.138	3.31	
								0.185	2.94	
Lu and Huang [17]	2013	$NaNO_3$: KNO_3 (60:40)	Al	13	---	heat-flux-type DSC	290-335 ℃	0.9	1.54	0.01 ~ 0.02
								2.7	1.44	
								4.6	1.37	
Lu and Huang [17]	2013	water	Al	90	---	heat-flux-type DSC	290-335 ℃	0.9	1.575	0.01 ~ 0.02
								2.7	1.49	
								4.6	1.45	

***** *SH stands for Specific Heat, DSC stands for Differential Scanning Calorimeter, T stands for Temperature.*

Table 3 contains the experimental results from eight papers. They tested the nanofluids in different combinations of nanoparticles and base fluids under different circumstances. It is hard to make a horizontal comparison of the nanofluids from different papers.

To intuitively illustrate the percentage change caused by the nanoparticles, several figures are plotted, as shown in Figure 7, 8, and 9. These figures show the percentage changes in the specific heat of various nanofluids as a function of the concentration of nanoparticles [14, 12, 17]. The percentage change is calculated as:

$$\text{Percentage change}=\frac{Measured\ nanofluid's\ specific\ heat - base\ fluid's\ specific\ heat}{base\ fluid's\ specific\ heat} \times 100 \quad (4)$$

The materials of the nanoparticles and base fluids are shown in the title, and separated by "/." In these figures, the plots all start from zero because at zero concentration, the nanoparticles have zero effect on the nanofluids. The plots indicate the decrease percentage of specific heat caused by adding the nanoparticles. Figure 7 shows the maximum decline of specific heat of base fluids happens in the nanofluid formed by 80-nm sized Al dispersed in engine oil. The specific heat of the nanofluid is reduced by up to 16.5%. Figure 8 shows that adding 21.7% Al_2O_3 into water decreases the water's specific heat up to 56.8%.

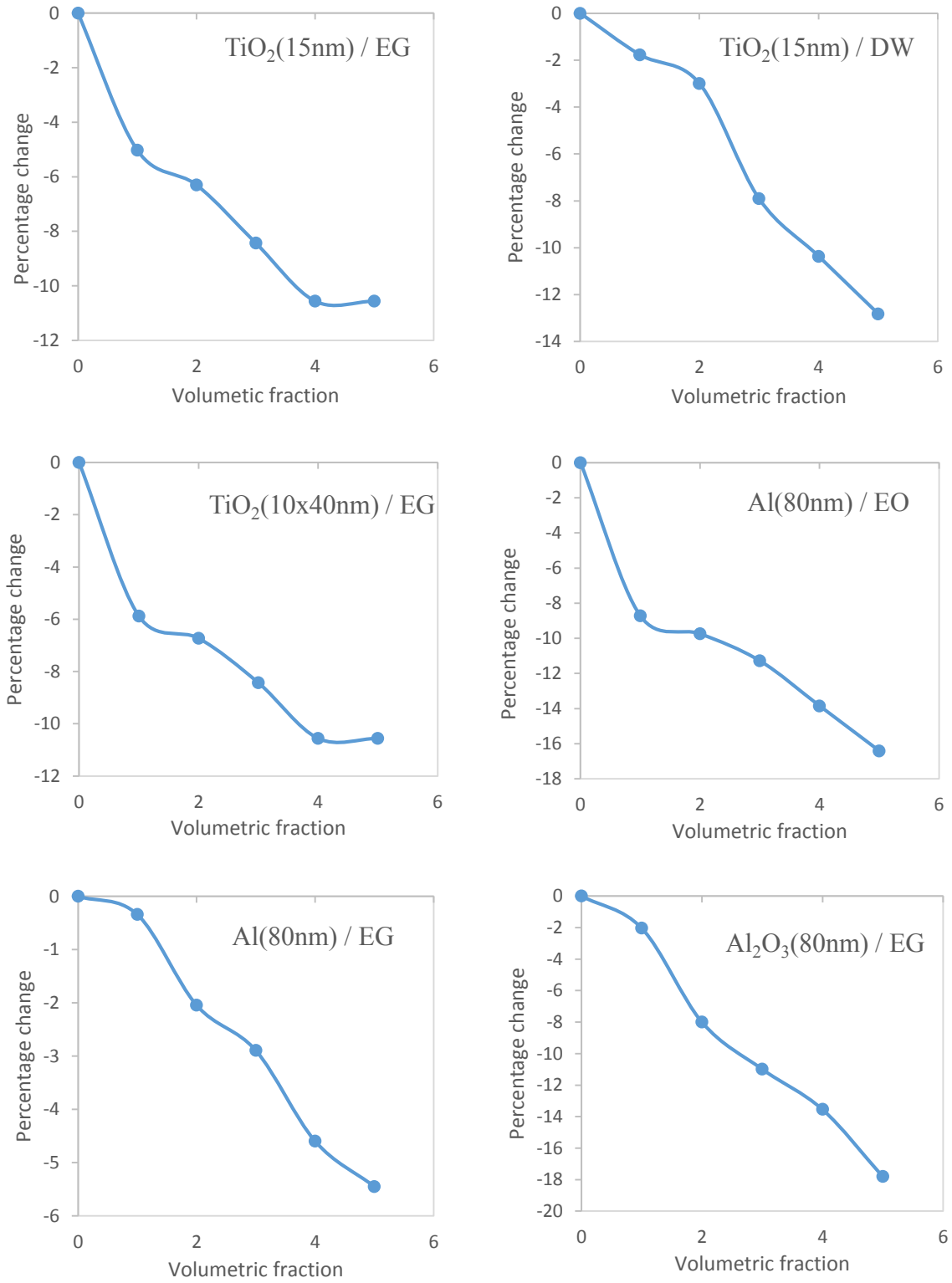

Figure 7. Percentage change in the specific heat of various nanofluids as a function of the volumetric fraction of nanoparticles [14]

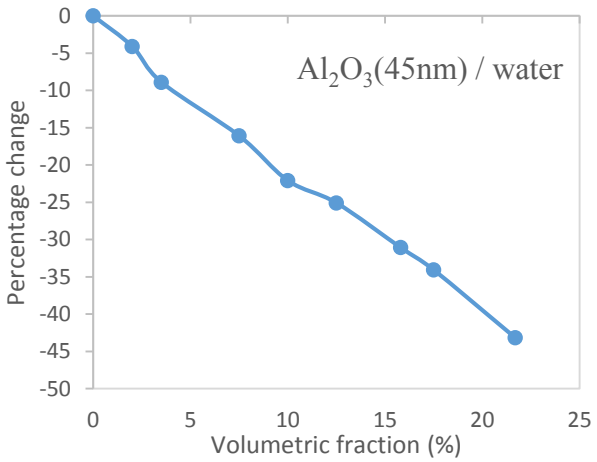

Figure 8. Percentage change in the specific heat of the nanofluid as a function of the volumetric fraction of Al_2O_3 nanoparticles [12]

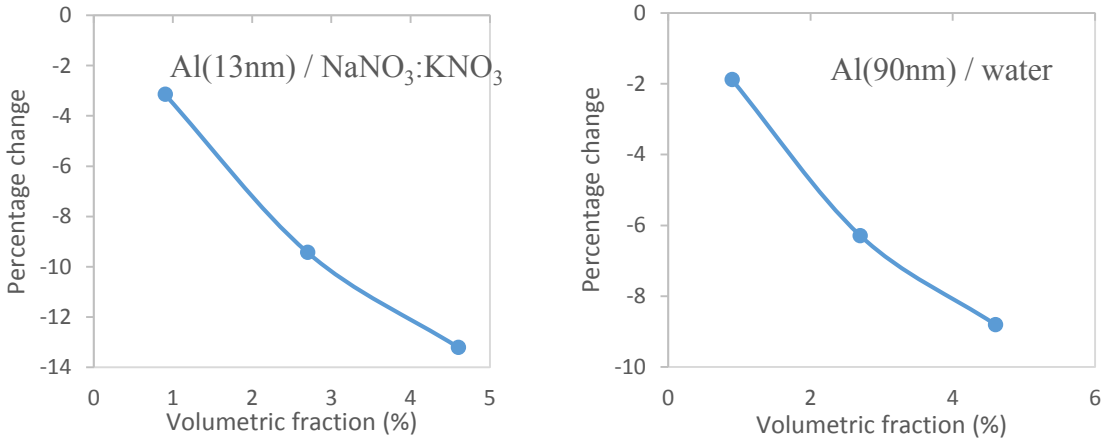

Figure 9. Percentage change in the specific heat of the nanofluids as a function of the volumetric fraction of different sized Al nanoparticles [17]

Basically, the authors of Table 3 show a decrease by adding nanoparticles. Additionally, Lu and Huang [17] demonstrated that larger sizes of nanoparticles lead to higher specific heat of nanofluids. Then Table 4 shows the maximum specific heat of nanofluids at certain concentrations of nanoparticles. The maximum specific heats from different authors happen at different concentrations of nanoparticles, which are below or around 1% mass concentration.

Table 4. Summary of experimental studies on specific heat of nanofluids - II

Author	Year	Base Fluid	Nano-particle	Particle Size (nm)	Nanofluid prepare	*SH Measurements	T (K)	Volume Fraction %	Nanofluid *SH ($kJ/kg \cdot K$)	Uncertainty cited in the publications
Chieruzzi et al. [19]	2013	$NaNO_3$: KNO_3 (60:40)	SiO_2	7	Hot plate method	DSC	300 ℃	0.5 (mass fraction)	1.329	±6%
								1.0 (mass fraction)	1.661	
								1.5 (mass fraction)	1.624	
Chieruzzi et al. [19]	2013	$NaNO_3$: KNO_3 (60:40)	Al_2O_3	3	Hot plate method	DSC	300 ℃	0.5 (mass fraction)	1.522	±6%
								1.0 (mass fraction)	1.745	
								1.5 (mass fraction)	1.590	
Chieruzzi et al. [19]	2013	$NaNO_3$: KNO_3 (60:40)	TiO_2	20	Hot plate method	DSC	300 ℃	0.5 (mass fraction)	1.390	±6%
								1.0 (mass fraction)	1.544	
								1.5 (mass fraction)	1.454	
Chieruzzi et al. [19]	2013	$NaNO_3$: KNO_3 (60:40)	SiO_2-Al_2O_3	2-200	Hot plate method	DSC	300 ℃	0.5 (mass fraction)	1.525	±6%
								1.0 (mass fraction)	2.018	
								1.5 (mass fraction)	1.673	

Table 4. continued

Author	Year	Base Fluid	Nano-particle	Particle Size (nm)	Nanofluid prepare	*SH Measurements	T (K)	Volume Fraction %	Nanofluid *SH ($kJ/kg \cdot K$)	Uncertainty cited in the publications
Shao [20]	2013	$NaNO_3$: KNO_3 (60:40)	Al_2O_3	---	Hot plate method	MDSC	350 ℃	0	1.47	±3.6%
								0.09	1.69	
								0.17	1.62	
								0.30	1.77	
								0.53	1.83	
								0.78	1.92	
								0.96	1.82	
								1.19	1.68	
Tiznobaik and Shin[21]	2012	Li_2CO_3: K_2CO_3 (62:38)	SiO_2	5	Hot plate method	modulated DSC	300 ℃	1 (mass fraction)	2.03(sample #1)	not found
									1.97(sample #2)	
									1.90(sample #3)	
Tiznobaik and Shin[21]	2012	Li_2CO_3: K_2CO_3 (62:38)	SiO_2	10	Hot plate method	modulated DSC	300 ℃	1 (mass fraction)	2.10(sample #1)	not found
									1.90(sample #2)	
									2.02(sample #3)	
Tiznobaik and Shin[21]	2012	Li_2CO_3: K_2CO_3 (62:38)	SiO_2	30	Hot plate method	modulated DSC	300 ℃	1 (mass fraction)	2.03(sample #1)	not found
									1.90(sample #2)	
									1.92(sample #3)	
Tiznobaik and Shin[21]	2012	Li_2CO_3: K_2CO_3 (62:38)	SiO_2	60	Hot plate method	modulated DSC	300 ℃	1 (mass fraction)	2.02(sample #1)	not found
									2.01(sample #2)	
									1.97(sample #3)	

Table 4. continued

Author	Year	Base Fluid	Nano-particle	Particle Size (nm)	Nanofluid prepare	*SH Measurements	T (K)	Volume Fraction %	Nanofluid *SH ($kJ/kg \cdot K$)	Uncertainty cited in the publications
Shin and Banerjee[18]	2011	chloride eutectics	SiO_2	26	Hot plate method	direct-synthesis method	560 ℃	1(mass fraction)	0.97 (#1) 1.00 (#2)	2% ~ 4%
Shin and Banerjee[22]	2011	Li_2CO_3 :K_2CO_3 (62:38)	Si	10	Hot plate method	DSC (ASTM-E1269)	560 ℃	1 (mass fraction)	1.98 (#1) 2.03 (#2) 1.93 (#3)	1% ~ 5%
Shin and Banerjee[23]	2013	Li_2CO_3 :K_2CO_3 (62:38)	Si	2-20	Hot plate method	DSC	560 ℃	1 (mass fraction)	1.97(fine powder #1) 1.81(fine powder #2) 1.77(fine powder #3) 1.18(coarse powder #1) 1.31(coarse powder #2) 1.29(coarse powder #3)	1.9% ~ 2.4%

** SH stands for Specific Heat, DSC stands for Differential Scanning Calorimeter.*

Figure10, 11, and 12 are plotted to analyze the effect on the specific heat of nanofluids by adding nanoparticles. Chieruzzi et al. [16] dispersed four types of nanoparticles into the same base salt mixture, which shows the maximum specific heat of nanfluids at 1 wt.%. SiO_2, Al_2O_3, and SiO_2-Al_2O_3 all increase the specific heat of the base salt mixture at 1 wt.% except that TiO_2 still decrease the specific heat of the base salt mixture even at 1 wt.%, as shown in Figure 10.

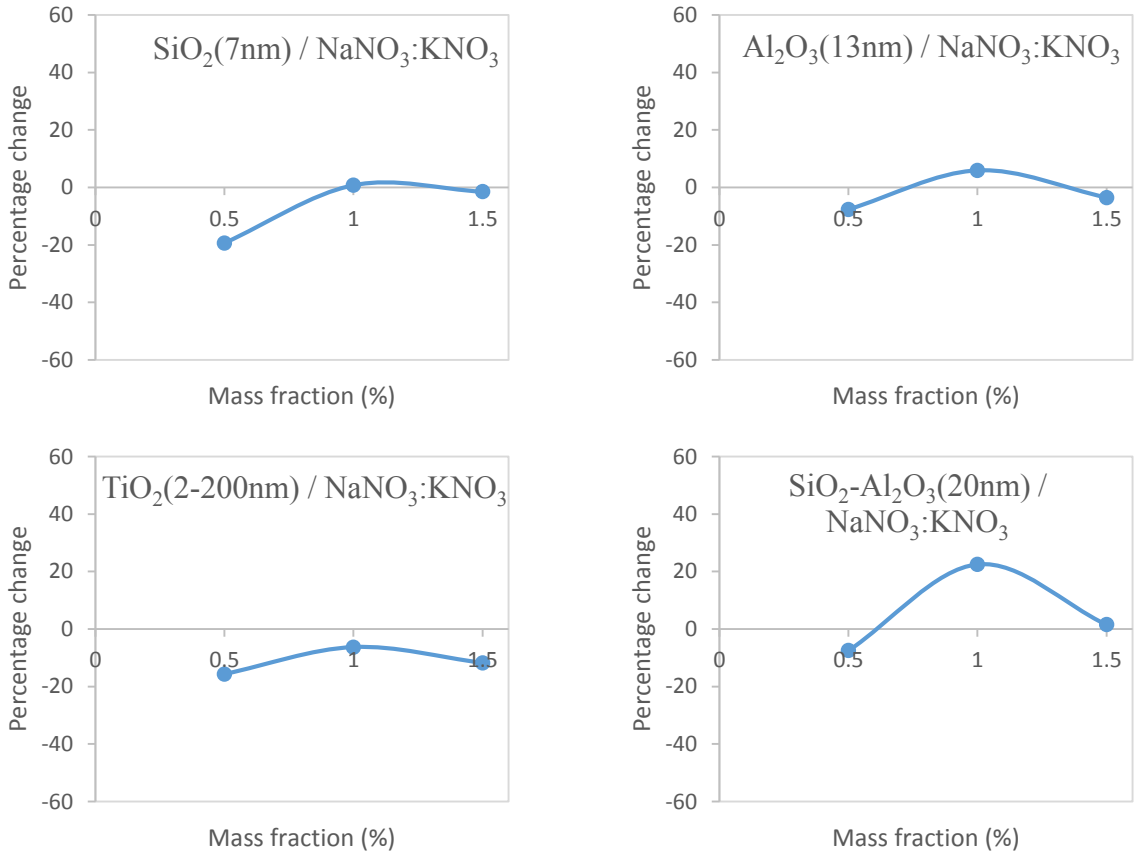

Figure 10. Percentage change in the specific heat of various nanofluids with the same base fluid and different nanoparticles as a function of the mass fraction of nanoparticles [16]

Tiznobaik and Shin [21] only tested the specific heat of nanofluids at 1% mass

fraction of nanoparticles. Four different sized Al nanoparticles were dispersed into the same molten salt eutectic. Figure 11 depicts the increased ratio of specific heat of nanofluids.

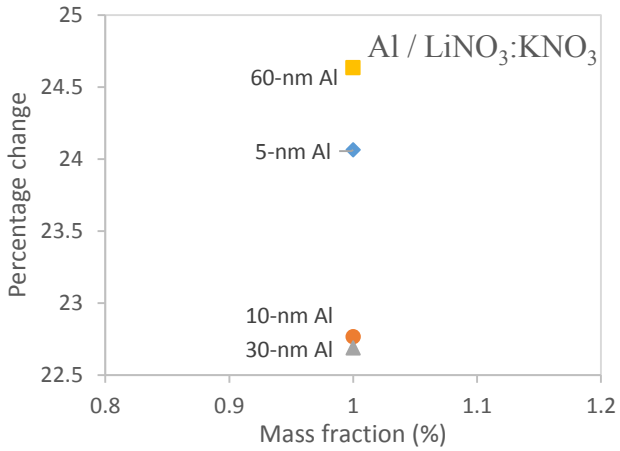

Figure 11. Percentage change in the specific heat of the nanofluid as a function of the mass fraction of different sized Al nanoparticles at 1 wt.% [21]

Figure 12 shows the percentage change in the specific heat of the $NaNO_3$:KNO_3 based nanofluid with Al_2O_3 as a function of the mass concentration of Al_2O_3 [20]. It is shown that adding different concentrations of Al_2O_3 nanoparticles into the base fluid all results in an increase of the specific heat.

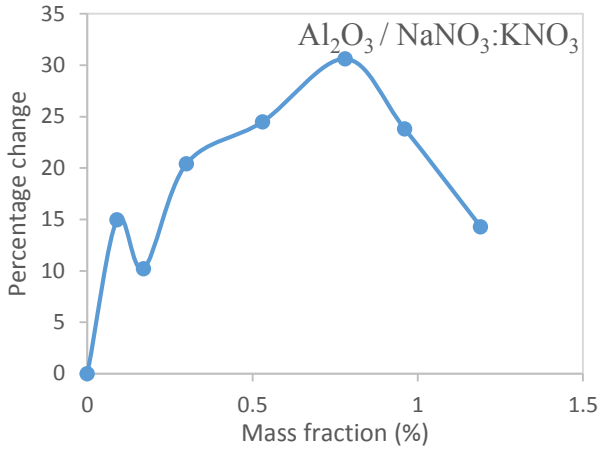

Figure 12. Percentage change in the specific heat of the nanofluid as a function of the mass fraction of different sized Al_2O_3 nanoparticles at 1 wt.% [20]

5.2 Overview of models for specific heat of nanofluids

To predict the specific heat as a function of the concentration of nanoparticles, different models were developed in the previous studies. They were used to compare with the experimental result. To illustrate the comparison, Table 5 was created for the models that were used to predict the specific heat of nanofluids; Table 6 was created for the models that were proposed to predict the specific heat of nanofluids with a parabolic shape. The comparisons of models and experimental result that are discussed in the same paper are also showing in Table 5 and Table 6. After Table 6, each model will be compared with selected sets of experimental result to verify if it is suitable for predicting all types of experimental result.

Table 5. Summary of models on specific heat of nanofluids - I

Author	Year	Model	Remark
Pak and Cho [10]	1998	$C_{p,nf} = \phi_{np} C_{p,np} + (1 - \phi_{np}) C_{p,f}$	No comparison between the experimental result and the model.
Murshed [14]	2011	$C_{p,nf} = \frac{\rho_{np}\phi_{np}C_{p,np} + \rho_f \phi_f C_{p,f}}{\rho_{np}\phi_{np} + \rho_f \phi_f}$	The model is in good agreement with the measurements in the paper.
Barbés [16]	2012	$C_{p,nf} = \frac{\rho_{np}\phi_{np}C_{p,np} + \rho_f \phi_f C_{p,f}}{\rho_{np}\phi_{np} + \rho_f \phi_f}$	The model is in good agreement with the measurements in the paper.
Zhou et al. [13]	2009	$C_{p,nf} = \phi_{np} C_{p,np} + (1 - \phi_{np}) C_{p,f}$ $C_{p,nf} = \frac{\rho_{np}\phi_{np}C_{p,np} + \rho_f \phi_f C_{p,f}}{\rho_{np}\phi_{np} + \rho_f \phi_f}$	The predictions of two models are used to compare with the experimental result. The first model fails to predict the experimental result, while the second one agrees with the experimental result.
Zhou and Ni[12]	2008	$C_{p,nf} = \phi_{np} C_{p,np} + (1 - \phi_{np}) C_{p,f}$ $C_{p,nf} = \frac{\rho_{np}\phi_{np}C_{p,np} + \rho_f \phi_f C_{p,f}}{\rho_{np}\phi_{np} + \rho_f \phi_f}$	The predictions of two models are used to compare with the experimental result. The first model fails to predict the experimental result, while the second one agrees with the experimental result.
O'Hanley et al. [15]	2011	$C_{p,nf} = \phi_{np} C_{p,np} + (1 - \phi_{np}) C_{p,f}$ $C_{p,nf} = \frac{\rho_{np}\phi_{np}C_{p,np} + \rho_f \phi_f C_{p,f}}{\rho_{np}\phi_{np} + \rho_f \phi_f}$	The predictions of two models are used to compare with the experimental result. The first model fails to predict the experimental result, while the second one agrees with the experimental result.
Lu and Huang [17]	2013	$C_{p,nf} = \frac{\rho_{np}\phi_{np}C_{p,np} + \rho_f \phi_f C_{p,f}}{\rho_{np}\phi_{np} + \rho_f \phi_f}$ $C_{p,nf} = \frac{C_{p,f}(\alpha - \alpha') + C_{p,m}\alpha'}{\alpha}$	The predictions of two models are used to compare with the experimental result. The first model fails to predict the experimental result, while the second one agrees with the experimental result.

Table 6. Summary of models on specific heat of nanofluids - II

Author	Year	Model	Remark
Chieruzzi et al. [19]	2013	$C_{p,nf} = \frac{\rho_{np}\phi_{np}C_{p,np}+\rho_f\phi_f C_{p,f}}{\rho_{np}\phi_{np}+\rho_f\phi_f}$	The model cannot predict the increase of nanofluilds' specific heat with the 1.0 wt.% of nanoparticles.
Shin and Banerjee[18]	2011	$C_{p,nf} = \frac{\rho_{np}\phi_{np}C_{p,np}+\rho_f\phi_f C_{p,f}}{\rho_{np}\phi_{np}+\rho_f\phi_f}$	The model cannot explain the anomalous enhancement of the specific heat at low concentrations of nanoparticles.
Tiznobaik and Shin [21]	2013	$C_{p,nf} = \frac{\rho_{np}\phi_{np}C_{p,np}+\rho_f\phi_f C_{p,f}}{\rho_{np}\phi_{np}+\rho_f\phi_f}$	The model cannot explain the observed enhancement in the nanofluids' specific heat
Shin and Banerjee[23]	2013	$C_{p,nf} = \frac{\rho_{np}\phi_{np}C_{p,np}+\rho_f\phi_f C_{p,f}}{\rho_{np}\phi_{np}+\rho_f\phi_f}$ $C_{p,nf} = \frac{\rho_{np}V_{np}C_{p,np} + \rho_c V_c C_{p,c} + \rho_f V_f C_{p,f}}{\rho_{np}V_{np} + \rho_c V_c + \rho_f V_f}$	The predictions of two models are used to compare with the experimental result. The first model fails to predict the experimental result, while the second one agrees with the experimental result.

From the above two tables, it is clear that some models have been repeated in many papers. The same model can be adopted to compare with different sets of experimental result. Through summarization, among all the published papers, only four different models of specific heat of nanofluids have been proposed.

The following sections will introduce these four models separately. The four models are named as Model I, Model II, Model III, and Model IV. These four models will be compared to determine if there is a unified model that predicts all the types of experimental result.

5.2.1 Model I

Model I is the simplest model and is similar to mixing theory for ideal gas mixtures, as shown in equation (5). Equation (5) has been used as a known formula in the assessment of the heat transfer performance of nanofluids in many papers [10, 12, 13, 15]. It is a direct average of specific heat values of the base fluid and the nanoparticles based of the volume fraction. Model I calculates the specific heat of nanofluids as:

$$C_{p,nf} = \phi_{np} C_{p,np} + (1 - \phi_{np}) C_{p,f} \tag{5}$$

Nanoparticle volume fraction is calculated by $\phi_{np} = \frac{V_{np}}{V_{np}+V_f}$ and base fluid volume fraction is $\phi_f = \frac{V_f}{V_{np}+V_f}$, thus $\phi_{np} + \phi_f = 1$.

5.2.2 Model II

The second model, as shown in equation (6), is the most commonly used. According to the literature review, more than 80% of papers adopt Model II. Model II is also the foundation of Model III and Model IV. Model II is based on the assumption of thermal equilibrium between the particles and the surrounding fluid. It excludes the effect of the interaction between the nanoparticles and the base fluid for the specific heat. Model II does not consider the change in specific heat of the base fluid or the nanoparticles after they combine. The density of nanofluids is defined as $\rho_{nf} = m_{nf}/V_{nf} = \phi_f \rho_f + (1-\phi_f)\rho_{np}$. Therefore, the specific heat of nanofluids is expressed as:

$$C_{p,nf} = \frac{\rho_{np}\phi_{np}C_{p,np}+\rho_f\phi_f C_{p,f}}{\rho_{np}\phi_{np}+\rho_f\phi_f} \quad (6)$$

Zhou et al. [13], Zhou and Ni [12] and O'Hanley [15] all compared Model I and Model II in their papers, and concluded that Model II is able to better predict the specific heat of nanofluids than Model I. Thus, only Model II will be used to verify if it is suitable for all the experimental result.

Model II shows an agreement with the experimental result from several published papers [12,13,14,15,16], which are all decreasing with the increased nanoparticles concentration. To verify if Model II is available for predicting all the experimental result, it is plotted to compare with Ref [17], as shown in Figure 13. The ratios of the predictions and the measurements are also plotted in Figure 13. Ref [17] shows the experimental result that are decreasing with the increased concentration.

However, Figure 13 shows that Model II cannot predict the experimental result from Ref [17], which means that Model II is not suitable for predicting all the specific heat of nanofluids that decreases with increased nanoparticles. Figure 13 clearly shows that Model II's prediction decreases when the fraction of nanoparticles increases, thus it cannot predict or verify the experimental result with a parabolic shape [19, 20, 22]. This indicates that Model II is not a unified model that can predict all the specific heat experimental result.

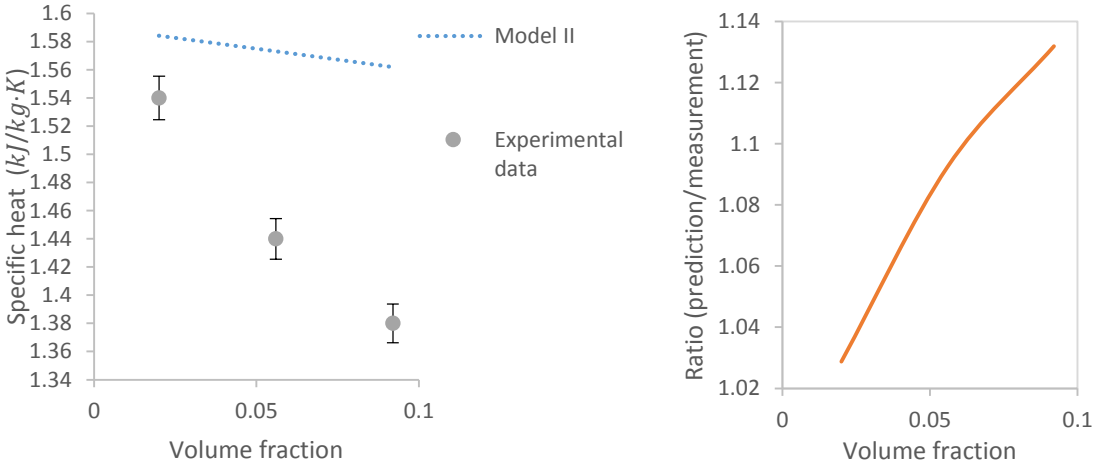

(a) 13nm sized $Al_2O_3/NaNO_3$-KNO_3

Figure 13. Prediction of Model II compared with Ref. [17]

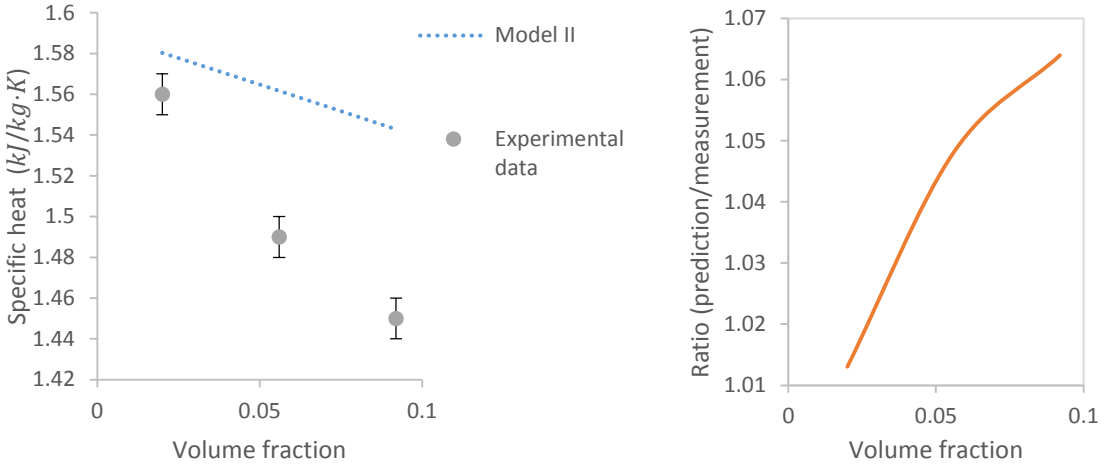

(b) 90nm sized Al_2O_3/$NaNO_3$-KNO_3

Figure 13. Continued

5.2.3 Model III

Both Model III and Model III are lack of the consideration of the interaction between the base fluids and the nanoparticles. To improve this, Lu and Huang [12], who introduced a "nanolayer" as a contribution into Model III, considered that the specific heat of a nanolayer ($C_{p,layer}$) is dependent on the size of nanoparticles or the combinations of nanoparticles and a base fluid. However, there is no experimental or theoretical result available for the nanolayer's specific heat ($C_{p,layer}$). The measured specific heat of a nanofluid ($C_{p,m}$) at a certain nanoparticles' concentration is a function of the specific heat of a nanolayer ($C_{p,layer}$):

$$C_{p,m} = \frac{C_{p,layer}W_{layer}+C_{p,np}W_{np}+C_{p,f}(W_f-W_{layer})}{W_{nf}} \quad (7)$$

The measured specific heat of a nanofluid ($C_{p,m}$) is a result of the superposition

of the specific heat of the nanolayer ($C_{p,layer}$), the nanoparticle ($C_{p,np}$), and the base fluid ($C_{p,f}$). Due to this, the specific heat of the nanolayer ($C_{p,layer}$) can be derived from Equation (7):

$$C_{p,layer} = \frac{C_{p,m}W_{nf} - C_{p,np}W_{np} - C_{p,f}(W_f - W_{layer})}{W_{layer}} \quad (8)$$

Once the specific heat of the nanolayer ($C_{p,layer}$) is known, the specific heat of the nanofluid ($C_{p,nf}$) at any nanoparticles' concentration is expressed as:

$$C_{p,nf} = \frac{C_{p,np}W'_{np} + C_{p,layer}W'_{layer} + C_{p,f}(W_f - W'_{layer})}{W'_{nf}} \quad (9)$$

Substituting the specific heat of the nanolayer ($C_{p,layer}$) from Equation (8) into Equation (9), the specific heat of the nanofluid ($C_{p,nf}$) at any nanoparticles' concentration can be obtained in Equation (10):

$$C_{p,nf} = \frac{C_{p,f}(\alpha - \alpha') + C_{p,m}\alpha'}{\alpha} \quad (10)$$

The relation between the volume fraction and mass fraction is:

$$\emptyset = \alpha^2\left(1 - \frac{\rho_f}{\rho_{np}}\right) + \alpha\left(\frac{\rho_f}{\rho_{np}}\right) \quad (11)$$

Figure 14 shows the predictions of Model III and Model II compared with the experimental result from Lu and Huang [17]. It shows that the predicted plots of Model III and Model II decrease continually, and Model II shows a larger deviation than Model

III. In Figure 14, the ratios of the calculated numbers from the models versus the experimental result are plotted to illustrate the deviation of each model. The ratio plots also indicate that Model III has a closer prediction than Model II. Thus, Model III appears to be a better predictor than Model II.

To verify if Model III is suitable to predict other author's experimental result, Model III is used to predict the experimental result published by Chieruzzi [19], as shown in Figure 15. The experimental result from Ref [19] reaches the maximum at 1% of nanoparticles, which is a typical distinction compared with the first type of experimental result.

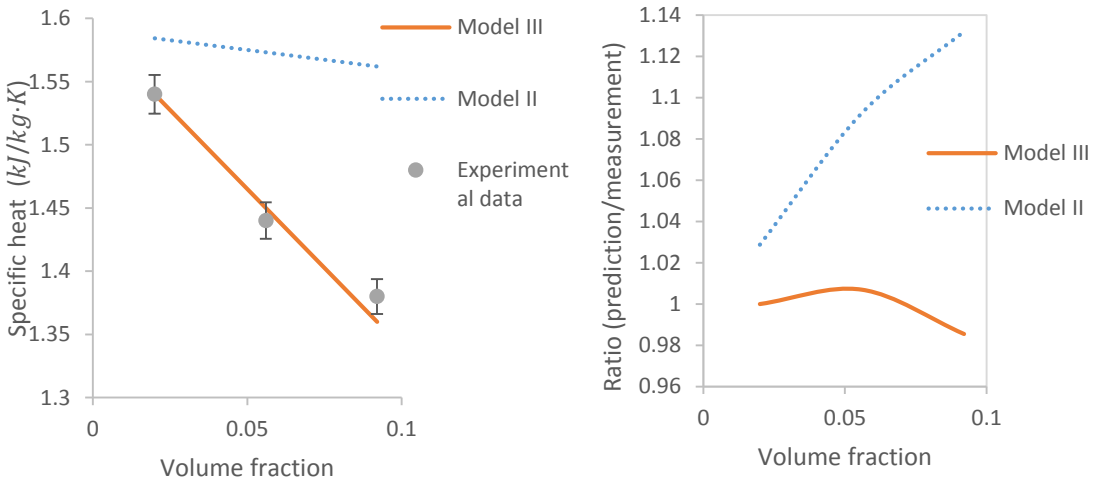

(a) 13nm sized $Al_2O_3/NaNO_3$-KNO_3

Figure 14. Predictions of Model II and Model III compared with Ref. [17]

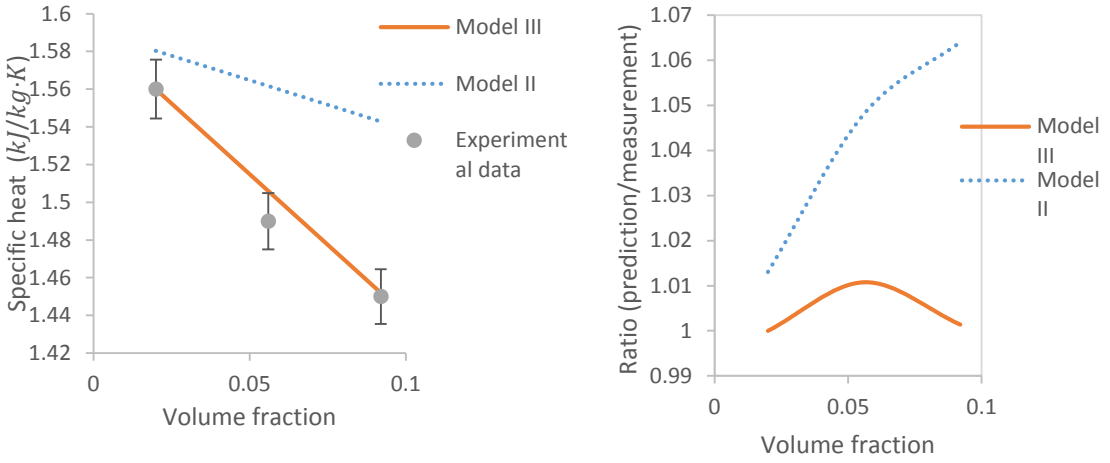

(b) 90nm sized Al_2O_3/$NaNO_3$-KNO_3

Figure 14. Continued

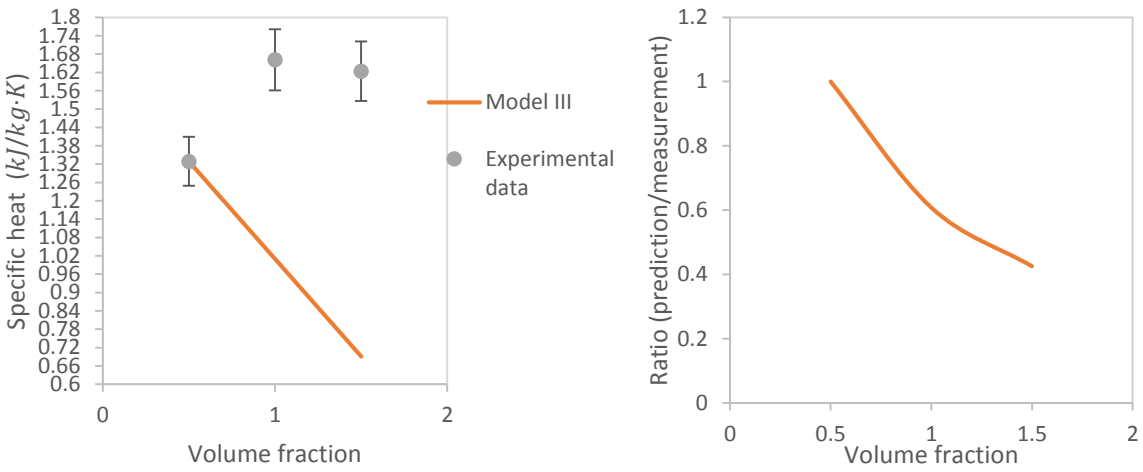

(a) 7nm sized SiO_2/ $NaNO_3$-KNO_3

Figure 15. Prediction of Model III compared with Ref. [19]

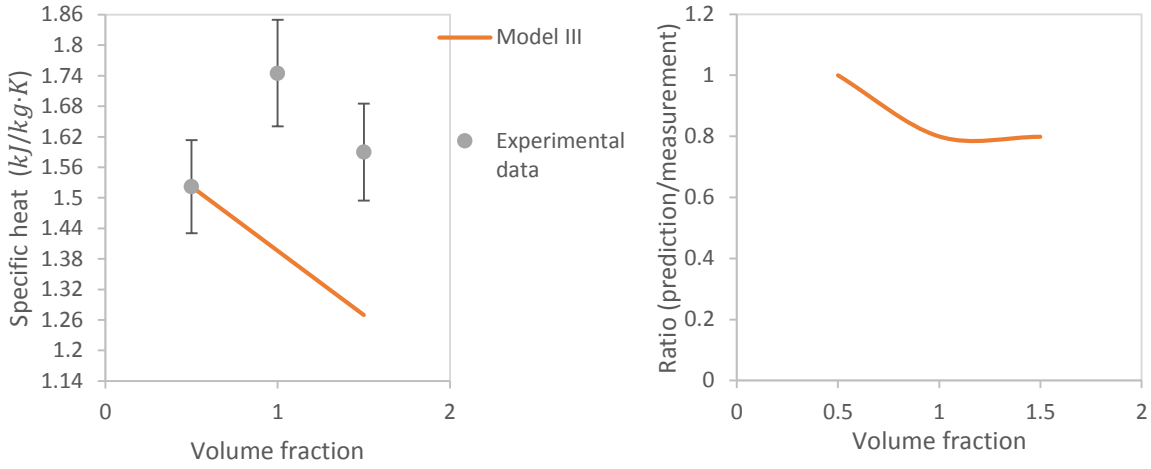

(b) 13nm sized Al_2O_3/ $NaNO_3$-KNO_3

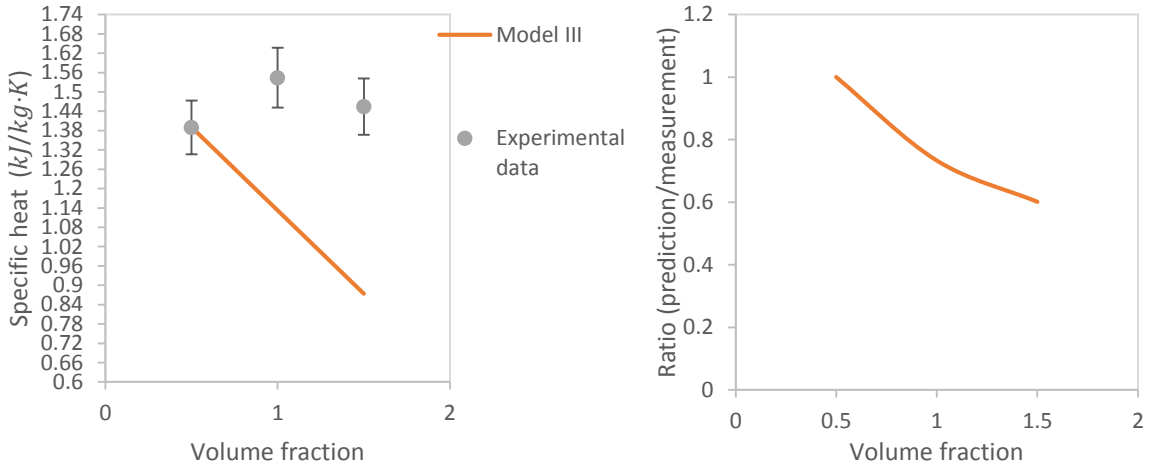

(c) 2~200nm sized TiO_2/ $NaNO_3$-KNO_3

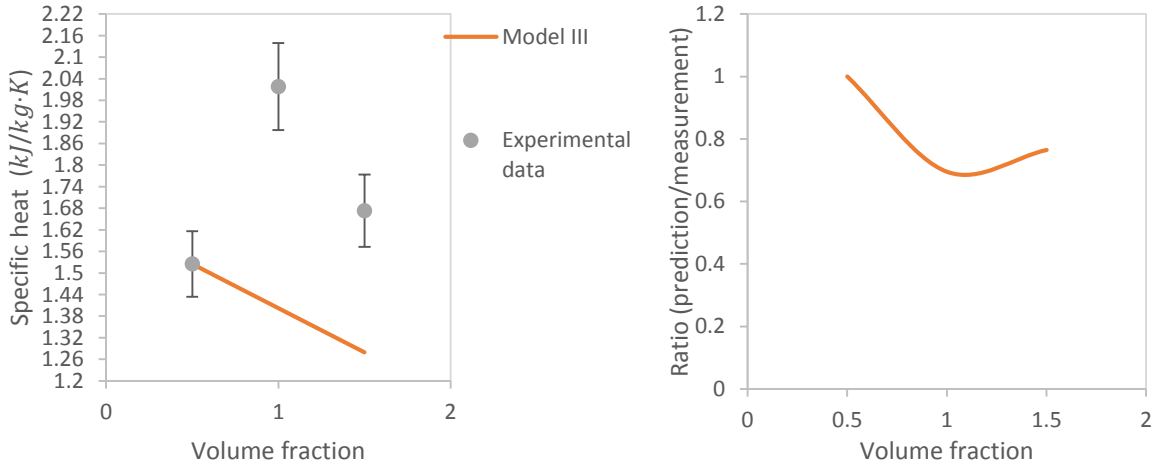

(d) 2~200nm sized SiO_2-Al_2O_3/ $NaNO_3$-KNO_3

Figure 15. Continued

In Figure 15, the prediction from Model III shows a large deviation with the experimental result, which indicates that Model III is not be able to predict other authors' experimental result. Thus, it is definitely not the case to determine that Model III is a unified model to predict all the experimental result.

Furthermore, there are also two restrictions in using Model III. First, in order to use Model III, at least one specific heat at a certain concentration of nanoparticles needs to be measured in an experiment. This measurement is required in equation (10) to calculate the specific heat at other concentrations. It is also the reason Figure 14 and Figure 15 show the same starting points instead of the prediction. Second, Model III can be only used to predict the specific heat of nanofluids with same sized nanoparticles instead of different sized nanoparticles [19]. These two restrictions show that Model III is limited, since it cannot independently predict without the measurement.

5.2.4 Model IV

Since none of Model Model I, Model II, and Model III could predict all the experimental result, IV was developed. It was proposed by Banerjee [23], and accounts for the contribution of the compressed phase to the total specific heat of nanomaterials. It is as follows:

$$C_{p,nf} = \frac{\rho_{np}V_{np}C_{p,np}+\rho_c V_c C_{p,c}+\rho_f V_f C_{p,f}}{\rho_{np}V_{np}+\rho_c V_c+\rho_f V_f} \quad (12)$$

The properties of the semisolid layer are the key issues required to use Model IV. However, Banerjee [23] pointed out that terms like the density, the volume fraction and

the specific heat of the semisolid compressed layer cannot be measured directly. Banerjee [23] assigned empirical numbers for these crucial terms. But his explanation was not specific, and his result was hard to replicate for other people. A 0.336J/g K of specific heat of nanofluids was calculated, which was far below Banerjee's calculation, 3.31 J/g K. Thus, Model IV is inappropriate to predict the specific heat of nanofluids.

6. EXPLANATIONS AND RECOMMENDATIONS

The previous models cannot successfully explain the observed change of the specific heat of nanofluids due to insufficient understanding of the basic mechanisms involved. Thus, this chapter outlines how the nanoparticles improve the specific heat of a base fluid at a nanoscale level. It focuses on explaining how nanoparticles contact with a base fluid at a nanoscale level. Two newly developed explanations are proposed to explicate the enhancement of specific heat. Furthermore, suggestions are proposed based on the new findings.

6.1 Explanations of the mechanisms of the variation of specific heat of nanofluids

Adding nanoparticles in a base fluid results in two types of experimental results of the specific heat of nanofluids. Since no consensus exists on the effect of adding nanoparticles on the specific heat in either experiments or theories, the explanations will be presented according to the two types of experimental results.

The first type of experimental result of the experimental result shows that nanfluid specific heat is decreasing when the nanoparticles concentration increases. This is because the nanoparticle has a relative lower specific heat than the base fluid. When the nanoparticles are added to the base fluid, they lower the mixing nanofluid's specific heat. Thus, the specific heat of the nanofluid is lower than the base fluid.

The second type of the experimental result shows that the specific heat of

nanofluids reaches its maximum at a low concentration of nanoparticles. The second type of experimental result is provided at a nanoscale level and results in an enhancement.

The researchers (Shin and Banerjee [15], Chieruzzi et al. [16]) who found the enhancement of the specific heat all stated in their papers that the formation of a nanolayer on the surface of the nanoparticle should be responsible for the enhancement of the specific heat of nanofluids. When nanoparticles disperse into the base fluid, both of their original states are destroyed. At the same time, the interaction between the nanoparticles' surfaces and the surrounding liquid molecules is considered. Some of the liquid molecules around the nanoparticles adhere to the surfaces to form layers. Chieruzzi et al. [19] also used SEM micrographs of the nanofluids at different concentrations of nanoparticles to prove the presence of an interaction between the nanoparticles and the base fluid. Oh [24] also demonstrated the existence of the nanolayer by presenting TEM images. The layer's thickness is 2-5 nm, which is about 10 molecules or less. Li [25] found that a thin layer of liquid is formed at the interface between the nanoparticle and liquid by tracking the atoms' positions.

The nanolayer between the nanoparticles and the base fluid is formed due to the unique characteristics of nanoparticles. Due to the nano-size of nanoparticles, they have high specific surface energies associated with the high surface area per unit mass. The larger surface energy results in an increased thermal resistance between the nanoparticles and the base fluid. The thermal resistance can be considered as thermal storage that stores the heat. The thicker the adhesion layer, the larger the thermal resistance will be,

which contributes to enhance the specific heat of nanofluids. Li [25] found that more attracted atoms form the layer around the nanoparticles when the diameters of the nanoparticles are larger. Therefore, the larger diameters of the nanoparticles lead to more significant enhancement of the thermal conductivity of the nanofluids. This is speculated, the specific heat of nanofluids is affected by the adhesion layer between the nanoparticles and the base fluid and is dominated by the thickness of the adhesion layer. For nanofluids, the unique feature of specific heat is caused by the small size of nanoparticle, and larger sizes increase specific heat. Lu and Huang [17] showed good corresponding results with this conclusion: comparing 13- and 90- Al nanoparticles, small size reduces the specific heat of nanofluid for a given volume fraction.

However, the above theory can only explain the enhancement of the specific heat, but cannot explain why the specific heat is lower above and below the concentration where the enhancement happens. To expand on the theory, two additional explanations are proposed based on.

6.2 Two novel explanations for the change of specific heat of nanofluids and recommendations

Before proposing the original explanations on a nanoscale level for the enhancement of specific heat, several concepts need to be introduced first.

The concepts of “lattice” and “phonon” are important to understand nanoscale theory. Atoms in a crystal are ordered based on image patterns and can be considered as dots. There are imagined linkages between the dots which are called “lattices.” The

lattice vibration waves are considered as "phonons." A phonon is a quantum of sound, that is, a quantized sound wave. It is a lowest energy, quantized state of a vibration within a lattice structure. They can be considered as particles that carry the lattice vibration energy. A phonon is a collective excitation in a period. The surface atoms in the lattices of a nanoparticle have less bonds and constraints than the inside ones. The energy between two objects is transferred by carriers such as phonons, electrons and fluid particles. The bonds between the atoms can be treated as a spring problem ($F = kx$). The surface atoms vibrate at a lower natural frequency and higher amplitudes, and generate potential energy in a harmonic approximation. The nanoparticle surface-to-volume ratio is larger the micro-sized particles, which causes surface energy to take a larger proportion.

6.2.1 First novel explanation for the change of specific heat of nanofluids

The following is the first proposed explanation of why the nanofluids' specific heat initially increases and then decreases. At a lower concentration of nanoparticles, there are not enough nanoparticles to adhere liquid molecules. Thus, little adhesion layers are formed, which lead to an enhancement of nanofluids' specific heat. As more nanoparticles are added into the base fluid, the specific heat increases. When the concentration of nanoparticles reaches the optimum value, the distance between two nanoparticles is the shortest length to avoid the effect of phonon scatterings from each other. With more nanoparticles in the nanofluid, the concentration of nanoparticles passes over the optimum value. Since the distance between two nanoparticles is shorter

than the optimum length, phonons scattering from each nanoparticle start to affect each other. This distance might be short enough to cancel or weaken the other nanoparticle's phonon scattering effect or atom vibration. Meanwhile, when two atoms come close to each other, their electrons begin to share orbitals. These phenomena will decrease the available degrees of freedom. Translation, rotation and the two types of energy, including potential energy and kinetic energy in vibration, represent the degree of freedom of motion which classically contributes to the heat of a thermodynamic system [26]. The loss of degrees of freedom weakens the specific heat of the nanofluid.

Based on these findings, an experimental suggestion is to add an additional process of measuring the molecules' forces in a nanofluid at different concentrations of nanoparticles. It is necessary to measure the specific heat and molecules' force at the same concentrations of nanoparticles. Then the relation between the measured specific heat and molecules' forces can be tracked. Since the distance between two atoms affects the molecules' forces, the relation of the specific heat and the distance between nanoparticles will be observed. This might be a reliable method to prove the proposed explanation and a more complete way to understand the interaction between the nanoparticles and the base fluid.

6.2.2 Second novel explanation for the change of specific heat of nanofluids

There is another proposed explanation of the change of specific heat of nanofluids. Specific heat quantifies the ability of a certain number of carries to store thermal energy. The energy is stored by a rise in the temperature of the carrier. Specific

heat of a metal can be expressed as a sum of specific heat of electrons and phonons. The phonons include acoustic and optical phonons. Acoustic phonons are similar to the way sound moves, so they are described as 'acoustic vibration.' We suppose that in a chain, the atoms bonded together by the lattice, the atoms vibrate along the wave propagation directions in the longitudinal and transverse modes [27]. Debye approximation (Debye, 1912) is a sine function to estimate the acoustic phonon specific heat:

$$w(K) \approx v_{g,ave}K \tag{13}$$

The acoustic phonon specific heat expressions equation (14) for low temperature and equation (15) for high temperature [26] are:

$$c_{v,D,3Dlow} \approx 234\eta_a\kappa_B\left(\frac{T}{\theta_D}\right)^3 \quad (T \ll \theta_D) \tag{14}$$

$$c_{v,D,3Dhigh} \approx 3\eta_a\kappa_B \quad (T \gg \theta_D) \tag{15}$$

where η_a is the number of unit cells per unit 'volume' of the given dimensionality, and η_a is true volume for 3D. κ_B is the Boltzmann's constant; θ_D is the Debye temperature. We can tell that for the high temperature, the acoustic phonon specific heat is independent from the temperature.

Optical phonon contribution is neglected for specific heat at low temperatures. In 1906, Einstein proposed a model that a single frequency assigned to each branch of the phonons causes flat dispersion vibration. While Debye's model is accurate to predict the specific heat of acoustic phonons, Einstein's model should be applied to the specific heat

of optical phonons. The electron specific heat calculated by Einstein's model is expressed as [26]:

$$c_{v,e} = \frac{\pi^2 \kappa_B^2 \eta_e}{2E_F} \tag{16}$$

Both phonons and electrons store energy through a distribution of energy state, which also is called energy level. Since phonons and electrons are governed by different distribution laws, such as the Bose-Einstein distribution and the Fermi-Dirac distribution law, respectively, a given state carries two electrons and unlimited phonons.

The interaction between the incoming and outgoing phonons is through a process known as Fermi's golden rule. The scattering rate increases with frequency as the phonon density of states increases. The scattering rate increases with temperature generally. The effective scattering rate is expressed as [26]:

$$\tau_{eff}^{-1} = 10^{10} s^{-1} + (10^{-17} s/K)\omega^2 T \tag{17}$$

For a 1D material, the thermal conductivity is:

$$\kappa_{1D} = \frac{1}{2\pi} \int_0^\infty \frac{v_g}{\tau^{-1}(\omega)} \hbar\omega \frac{\partial f_{BE}^0}{\partial T} d\omega \tag{18}$$

There are three typical types of phonon scattering processes. Type 1 is two incoming phonons scattering into a third while conserving energy and momentum. Type 2 is one phonon decaying into two outgoing phonons while conserving energy and momentum. Type 3 is two incoming phonons scattering into a third while conserving

energy but not momentum [26]. A U process is similar to type 1 of the scattering process of two incoming and one outgoing phonons. When temperature increases, U process scattering becomes dominant and the specific heat begins to asymptote toward a constant value. As temperature increases further, the scattering rate continues to rise, resulting in a decrease in thermal conductivity.

The second proposed explanation of nanofluids' specific heat change is obtained from the above equations. Based on the observation through the above equations, when the status (s) changes from zero to infinity, the specific heat of nanofluid first increases and then decreases.

It is not hard to tell in equation (17) that the scattering effective rate is effected by the terms of phonon wavevector (K), natural frequency (ω) and status (s). If the wavevecter and natural frequency are assumed to stay at certain constants, then effective scattering rate (τ_{eff}^{-1}) first decreases then increases as the status changes from zero to infinity. When effective scattering rate decreases, thermal conductivity (κ) from equation (18) increases, which leads the specific heat values of electrons (equation (16)) and phonons (equation (15)) to increase. The specific heat of the electrons and phonons assemble the specific heat of a nanofluid. Therefore, the specific heat of a nanofluid increases with the effective scattering rate decreasing. In contrast, as the effective scattering rate increases, the specific heat value will decrease. The peak of nanofluid specific heat occurs at the critical status.

In order to prove the above explanation, more calculations are needed for equations (13) to (18). If the number of the critical status can be calculated, it will be

easier to predict the peak value of specific heat and prove the explanation is reasonable. This will help improve better understanding, and even allow the prediction, of the change of specific heat. From equation (17), it is seen that the increased temperature results in an increase in the effective scattering rate. Both of the proposed explanations mention the scattering effect, it is also interesting to know the relation between the temperature and the scattering effect.

7. FINDINGS AND CONCLUSIONS

Based on the research, several findings are listed below:

1. Two types of experimental results of the specific heat of nanofluids have been discovered. The first type is that the specific heat of nanofluids decreases consistently when adding nanoparticles. The second type is that the specific heat of nanofluids first increases, then decreases after reaching the maximum.

2. Four different models that predict the change of specific heat of nanofluids from the previous studies have been summarized. None of them are able to adequately predict all the experimental results.

3. A theory at a nanoscale level that can only explain the enhancement of the specific heat of nanofluids was outlined. However, it cannot predict the trend of the specific heat of nanofluids.

4. Thus, two novel explanations at the nanoscale level predicting the trend of the specific heat of nanofluids have been proposed.

Considering all the findings of the research project, several conclusions can be drawn:

1. No agreement has been reached on the previous experimental results of the specific heat of nanofluids.

2. A unified model or explanation that is able to adequately predict the change of specific heat of a nanofluid of concentrations of nanoparticles does not appear to exist. No existing model is able to verify the experimental data of nanofluids' specific heat.

3. There does not seem to be a unified explanation for the change of the specific heat of nanofluids.

8. RECOMMENDATIONS FOR FUTURE RESEARCH

Three recommendations for future research on nanofluids' specific heat are listed below:

1. A factorial experiment is necessary to evalute the effects on nanofluids of various factors such as nanoparticle size, nanoparticle and nanofluid materials, and nanofluid's specific heat measurement method.

2. It is necessary to add an additional process of measuring the molecules' forces in a nanofluid at different concentrations of nanoparticles in experiments. This might be a reliable method to prove the proposed explanations in a better way to understand the interaction between the nanoparticles and the base fluid.

3. In order to gain better understanding, and to predict the change of specific heat, more calculations need to be taken on the equations mentioned in Chapter 5: the value of the critical status, where the optimal specific heat happens can be calculated, and this method can be used to precisely predict the peak value of the specific heat and its optimal concentration.

4. It is interesting to track the relation between the temperature and the scattering effect of nanofluids.

REFERENCES

1. Wong, Kaufui V., and De Leon, Omar, 2010, *Applications of Nanofluids: Current and Future*, Advances in Mechanical Engineering 2010.
2. Saidur, R., Leong, K. Y., and Mohammad, H. A., 2011, "A Review on Applications and Challenges of Nanofluids," Renewable and Sustainable Energy Reviews, **15**(3), pp. 1646-1668.
3. Das, Sarit K., Choi, Stephen U. S., Yu, Wenhua, and Pradeep T., 2008, *Nanofluids: Science and Technology*, Wiley, New York.
4. Micro & Nano Technology, 2014, from http://www.particlesciences.com/services/micro-nano-technology/
5. Kostic, M., Golubovic, M., Hull, J. R., and Choi, S.U.S., 2010, "One-Step Method for the Production of Nanofluids," U.S. Patent No. 7,718,033 B1.
6. Wikipedia, 2014, Differential Scanning Calorimetry, from http://en.wikipedia.org/wiki/Differential_scanning_calorimetry
7. Biochembayern, 2013, "Differential scanning Calorimetry," from http://biochembayern.wordpress.com/2013/03/26/differential-scanning-calorimetry/
8. Wikipedia, 2014, Scanning electron microscope, from http://en.wikipedia.org/wiki/Scanning_electron_microscope
9. Choi, S. U., and Eastman, J. A., 1995, "Enhancing Thermal Conductivity of Fluids with Nanoparticles," Argonne National Lab., IL, United States, 231, pp.99-106.

10. Pak, B. C., and Cho, Y. I., 1998, "Hydrodynamic and Heat Transfer Study of Dispersed Fluids with Submicron Metallic Oxide Particles," Experimental Heat Transfer an International J., **11**(2), pp.151-170.
11. Namburu, P. K., Kulkarni, D. P., Dandekar, A., and Das, D. K., 2007, "Experimental Investigation of Viscosity and Specific Heat of Silicon Dioxide Nanofluids," Micro & Nano Letters, IET, **2**(3), pp.67-71.
12. Zhou, S. Q., and Ni, R., 2008, "Measurement of the Specific Heat Capacity of Water-Based Al_2O_3 Nanofluid," Applied Physics Letters, **92**(9), 093123-093123.
13. Zhou, L. P., Wang, B. X., Peng, X. F., Du, X. Z., and Yang, Y. P., 2009, "On the Specific Heat Capacity of CuO Nanofluid," Advances in Mechanical Engineering, **2010**(4).
14. Murshed, S. M. S., 2011, "Simultaneous Measurement of Thermal Conductivity, Thermal Diffusivity, and Specific Heat of Nanofluids," Heat Transfer Engineering, **33**(8), pp.722-731.
15. O'Hanley, H., Buongiorno, J., McKrell, T., and Hu, L. W., 2012, "Measurement and Model Validation of Nanofluid Specific Heat Capacity with Differential Scanning Calorimetry," Advances in Mechanical Engineering.
16. Barbés, B., Páramo, R., Blanco, E., Pastoriza-Gallego, M. J., Piñeiro, M. M., Legido, J. L., and Casanova, C., 2013, "Thermal Conductivity and Specific Heat Capacity Measurements of Al_2O_3 Nanofluids," J. of Thermal Analysis and Calorimetry, **111**(2), pp.1615-1625.

17. Lu, M. C., and Huang, C. H., 2013, "Specific Heat Capacity of Molten Salt-Based Alumina Nanofluid," Nanoscale Research Letters, **8**(1), pp.1-7.
18. Shin, D., and Banerjee, D., 2011, "Enhancement of Specific Heat Capacity of High-Temperature Silica-Nanofluids Synthesized in Alkali Chloride Salt Eutectics for Solar Thermal-Energy Storage Applications," International J. of Heat and Mass Transfer, **54**(5), pp. 1064-1070.
19. Chieruzzi, M., Cerritelli, G. F., Miliozzi, A., and Kenny, J. M., 2013, "Effect of Nanoparticles on Heat Capacity of Nanofluids Based on Molten Salts as PCM for Thermal Energy Storage," Nanoscale Research Letters, **8**(1), pp.448.
20. Shao, Q., 2013, "The Effect of Nanoparticle Concentration on Thermo-Physical Properties of Alumina-Nitrate Nanofluid," M.S. thesis, Texas A&M University.
21. Tiznobaik, H., and Shin, D., 2013, "Enhanced Specific Heat Capacity of High-Temperature Molten Salt-Based Nanofluids," International J. of Heat and Mass Transfer, **57**(2), pp.542-548.
22. Shin, D., and Banerjee, D., 2011, "Enhanced Specific Heat of Silica Nanofluid," J. of Heat Transfer, **133**(2), 024501.
23. Shin, D., and Banerjee, D., 2013, "Enhanced Specific Heat Capacity of Nanomaterials Synthesized by Dispersing Silica Nanoparticles in Eutectic Mixtures," J. of Heat Transfer, **135**(3), 032801.
24. Oh, S. H., Y. Kauffmann, C. Scheu, W. D. Kaplan, and M. Rühle, "Ordered Liquid Aluminum at the Interface with Sapphire," Science, **310**(5748), pp. 661-663.

25. Li., L., Zhang, Y., Ma, H., and Yang, M., 2010, "Molecular Dynamics Simulation of Effect of Liquid Layering around the Nanoparticle on the Enhanced Thermal Conductivity of Nanofluids," J. of Nanoparticle Research, **12**(3), pp.811-821.
26. Fisher, S.T., 2003, *Thermal Energy at the Nanoscale*, World Science, Purdue University, USA, Chap. 5.
27. Fisher, S.T., 2003, *Thermal Energy at the Nanoscale*, World Science, Purdue University, USA, Chap. 3.